SunQM-6s8: {N,n} QM Field Theory Development on the E/RFe-force, the G/RFg-force, and the Spin-spin Interaction

Yi Cao
e-mail: yicaojob@yahoo.com. ORCID: 0000-0002-4425-039X

Abstract

The foundation of a brand new {N,n} QM field theory has been established in the articles of SunQM-6, -6s1, -6s2, -6s3, and -6s4. In the current article, I added some new developments. 1) For either an E/RFe-force field or a G/RFg-force field, or the spinning of a force field, we can use |n,*l*,m> QM state to describe, and then we can simplify the description by using nLL and nL0 QM modes only, or even by using n = 2 (with |2,1,0> and |2,1,±1>) for the description; 2) Alternatively, for a static force field (including either the G-force, or RFg-force, E-force, or RFe-force field), we can use n = 1 QM state |1,0,0> to describe. When this G-force field (or RFg-force, or E-force, or RFe-force field) increases the speed of either the translational motion or the spin motion, we can use the higher n number of nLL/nL0 mode to describe. 3) Based on that, either a single pair of E/RFe-force, or two pairs of E/RFe-force in turns of spin-spin interaction, or a single pair of G/RFg-force, or two pairs of G/RFg-force in turns of spin-spin interaction, was analyzed; 4) That the Moon is slowly moving away from the Earth can be re-explained as the weakening of the parallel spin-spin attractive force between them; 5) A complete description for the nLL QM-force was given, it not only includes the QM force in θ-1D that forming a disk (from a sphere), but also includes the QM force in Δr-1D that dissecting a disk into several rings; 6) the formation of the two spiral arms of a galaxy can be explained by using the "|nL0> elliptical/parabolic/hyperbolic orbital model". Finally, because of its completeness and self-consistence, I do believe that the {N,n} QM is qualified to be put into the "Feynman Pool" as one of the many co-existing QM theories.

Key Words: Quantum mechanics, {N,n} QM field theory, Schrodinger equation, spin-spin interaction.

Introduction

In August 2016, I discovered that the Solar system follows a brand new {N,n//6} quantum mechanical structure [1]. Based on that result, (during the 10 years of the closed-door research), I further (independently) developed the {N,n} QM theory, and showed that not only the formation of Solar system [1] ~ [16], but also the formation of the whole universe [17] ~ [25], may can be described by the {N,n} QM. (Note: As an independent scientist, some of my research work may belong to a citizen scientist leveled work). As part of the {N,n} QM development, I (independently) designed and developed a brand new {N,n} QM field theory [23] ~ [24], [26] ~ [31]. The foundation of this theory includes: the four fundamental forces (Gravity, Electromagnetic, Strong, Weak, abbreviated as G-, E/M-, S-, W-forces) have been re-classified into three pairs of force (E/RFe-force, G/RFg-force; S/RFs-force, see SunQM-6); all point-centered fields (including the mass field, the force field, and the energy field) can be represented by the Schrodinger equation/solution (in form of non-Born probability as well as in the form of 3D spherical wave packet, see SunQM-6s4); the non-Born probability description (that equals to the re-explanation of the Born probability density) as the collection of all elliptical orbital tracks (or, the Born probability density map's contour lines can be re-explained as the trajectory of the motion electron, see SunQM-6s2's Fig-2), the spherical 3D wave packet description and the dis-entanglement of the outmost shell (i.e., the "general decaying" process, see SunQM-6s1, -6s2, -6s3), the "|nL0> elliptical/parabolic/hyperbolic orbital transition model" (see SunQM-6s2, -6s3), and the trick that

using the high-frequency n' quantum number to pin-point any small region in the {N,n} QM field (see SunQM-3s11, -6s1, etc.). In the current paper, I presented some new detailed developments on the {N,n} QM field theory. Note: The current article (SunQM-6s8) was drafted before SunQM-6s4, SunQM-6s5, SunQM-6s6, and SunQM-6s7. So, some of the explanations may be still in the old way (in comparison with those later articles).

Note: QM means Quantum Mechanics. For {N,n} QM nomenclature as well as the general notes, please see SunQM-1's sections VII & VIII. Note: Microsoft Excel's number format is often used in this paper, for example: x^2 = x^2, 3.4E+12 = $3.4*10^{12}$ = 3.4×10^{12}, 5.6E-9 = $5.6*10^{-9}$. Note: The easiest reading sequence for the (31 posted) SunQM series papers is: SunQM-1, 1s1, 1s2, 1s3, 2, 3, 3s1, 3s2, 3s6, 3s7, 3s8, 3s3, 3s9, 3s4, 3s10, 3s11, 4, 4s1, 4s2, 5, 5s1, 5s2, 7, 6, 6s1, 6s2, 6s3, 6s4, 6s5, 6s6 and 6s7. Note: for all SunQM series papers, reader should check "SunQM-9s1: Updates and Q/A for SunQM series papers" for the most recent updates and corrections. Note: |n*l*m> means |n,*l*,m> QM state, "nLL" or |nLL> means |n,*l*,m> QM state with *l* = n-1 = L, and *m* = n-1 = L. "nL0" or |nL0> means |n,*l*,m> QM state with *l* = n-1 = L, and m = 0. Note: In the current paper, the cited SunQM series numbers of those pre-posted SunQM papers may not be the final SunQM series numbers (after posting), so, readers may need to match the right SunQM series number (for those pre-posting SunQM papers after they are posted, according to the list of "A series of SunQM papers that I am working on" at the end of current paper) before reading those (pre-posted) citations.

I. One single pair of E/RFe-force: New development on a translating and/or spinning charge's |n,*l*,m> mode in the {N,n} QM field theory.

I-a. For a spinning E/RFe-force field, the vector decomposition of $\vec{\mathbf{E}} = \overrightarrow{\mathbf{E}_r} + \overrightarrow{\mathbf{E}_\varphi}$ gives $\overrightarrow{\mathbf{E}_r}$ correlating to nL0 mode, and $\overrightarrow{\mathbf{E}_\varphi}$ correlating to nLL mode

Although my goal is to use Schrodinger equation/solution and |n,l,m> QM (i.e., using nL0 mode and nLL mode, see SunQM-6) to describe the E/RFe-force field, here, let's first used the vector decomposition (i.e., an old and simpler way in classical physics) to explain the nL0 mode vs. nLL mode for the E-force vector $\vec{\mathbf{E}}$. In SunQM-6s1's Fig-1a, in an H-atom, a $\overrightarrow{\mathbf{E}_r}$ vector is formed from the positive proton to the negative electron, when an electron doing the circular orbital movement in xy-plane (from +x axis to +y axis), the spinning of $\overrightarrow{\mathbf{E}_r}$ vector produces the $\overrightarrow{\mathbf{E}_\varphi}$ component (also from +x axis to +y axis). (Notice that this perfectly matches to "the face-to-face tidal-locked binary circular orbital rotation" model between the proton and the electron, see SunQM-6s7). Using the vector decomposition, we can obtain $\vec{\mathbf{E}} = \overrightarrow{\mathbf{E}_r} + \overrightarrow{\mathbf{E}_\varphi}$ as shown in Figure 1. When the spin vector $\overrightarrow{\mathbf{s}_z} << \infty$, both $\overrightarrow{\mathbf{E}_r} > 0$ and $\overrightarrow{\mathbf{E}_\varphi} > 0$ (see Figure 1a). However, I assumed that when the spin vector $\overrightarrow{\mathbf{s}_z} \to \infty$, $\overrightarrow{\mathbf{E}_\varphi} \to$ maximum and $\overrightarrow{\mathbf{E}_r} \to 0$ (see Figure 1b). From the previous {N,n} QM developments, now we know that for a static E-force field's $\vec{\mathbf{E}}$ vector, it is in nL0 mode (if we want to use |n,*l*,m> QM state to describe it). Because the static $\vec{\mathbf{E}}$ has $\overrightarrow{\mathbf{E}_\varphi} = 0$, which means $\vec{\mathbf{E}} = \overrightarrow{\mathbf{E}_r}$, thus $\overrightarrow{\mathbf{E}_r}$ must be in nL0 mode. Consequently, $\overrightarrow{\mathbf{E}_\varphi}$ must be in nLL mode.

So, for a real spinning E-force field's $\vec{\mathbf{E}}$ vector, it may usually contain both nL0 mode (for $\overrightarrow{\mathbf{E}_r}$ component) and nLL mode (for $\overrightarrow{\mathbf{E}_\varphi}$ component). Using QM terminology, a spinning $\vec{\mathbf{E}}$ is usually in the superposition of nL0 mode and nLL mode. The faster the spin speed of the $\vec{\mathbf{E}}$, the more percentage of $\vec{\mathbf{E}}$ in nLL mode, and less percentage in nL0 mode. Suppose in a case we have 90% $\vec{\mathbf{E}}$ in nL0 mode, and 10% $\vec{\mathbf{E}}$ in nLL mode, in the rest part of section I, we only analyze the 10% $\vec{\mathbf{E}}$ that in the pure nLL mode (i.e., how it behaviors and how the correlated companion RFe-force vector behaviors). Because $\vec{\mathbf{E}}$ is naturally in nL0 mode, in SunQM-6s5, we sometimes call the nLL mode $\vec{\mathbf{E}}$ (i.e., the $\overrightarrow{\mathbf{E}_\varphi}$ component that is in nLL mode) as the "**inversed $\vec{\mathbf{E}}$** ", or the "reversed $\vec{\mathbf{E}}$ ", to distinguish it from the natural nL0 mode $\vec{\mathbf{E}}$ (i.e., the $\overrightarrow{\mathbf{E}_r}$ component). (Note: Duo to my poor English, here both the "inversed $\vec{\mathbf{E}}$" or the "reversed $\vec{\mathbf{E}}$" means the same thing).

We may use $\overrightarrow{\mathbf{RFe}}$ vector to represent the RFe-force (circular) vector for the analysis. Similarly, due to that the natural RFe-force is in nLL mode (caused by the natural static $\vec{\mathbf{E}}$ in nL0 mode), and can be changed to be nL0 mode when the $\vec{\mathbf{E}}$ is inversed (by spinning), thus, we may also call the nL0 mode $\overrightarrow{\mathbf{RFe}}$ as the "**inversed $\overrightarrow{\mathbf{RFe}}$**" (or the "reversed $\overrightarrow{\mathbf{RFe}}$") to distinguish it from the natural nLL mode $\overrightarrow{\mathbf{RFe}}$. Then, the magnetic force $\vec{\mathbf{B}}$ vector can be either the natural RFe-force in nLL mode, or the inversed RFe-force in nL0 mode. (Note: for the inversed RFe-force in nL0 mode, sometimes we also call it "nL0 QM-force").

For the $\vec{\mathbf{B}}$ vector in nL0 mode, it is a nL0 QM-force in pseudo z-1D and spread out (a little bit) in xy-2D (that is why we call it pseudo z-1D, also see SunQM-6s1's Fig-5c). If $\vec{\mathbf{E}}$ vector spins max ($\overrightarrow{s_z} \to \infty$), then $\vec{\mathbf{E}}$ vector become 100% $\overrightarrow{\mathbf{E}_\varphi}$, or it become a pure φ-1D circular force vector, no z-component, and then $\vec{\mathbf{B}}$ vector become a pure z-1D vector (or a true z-1D vector, because it has no spread out in xy-2D).

This analysis may lead to a simple picture: by default, a point positive charge's static electric field vector has $\vec{\mathbf{E}} = \overrightarrow{\mathbf{E}_r}$, with $\overrightarrow{\mathbf{E}_\varphi} = \mathbf{0}$; and a photon's electric field vector has $\vec{\mathbf{E}} = \overrightarrow{\mathbf{E}_\varphi}$, with $\overrightarrow{\mathbf{E}_r} = \mathbf{0}$. (Note: Alternatively, a photon's $\vec{\mathbf{E}} = \overrightarrow{\mathbf{E}_r} + \overrightarrow{\mathbf{E}_\varphi}$ may also can be described as an outward-spiral, as shown in SunQM-6s5's Fig9c).

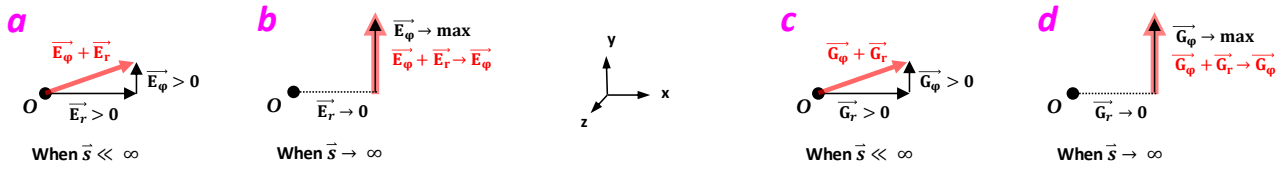

Figure 1a (and Figure 1b). Illustration of the vector decomposition of $\vec{\mathbf{E}} = \overrightarrow{\mathbf{E}_r} + \overrightarrow{\mathbf{E}_\varphi}$ for a spinning E/RFe-force field.
Figure 1c (and Figure 1d). Illustration of the vector decomposition of $\vec{\mathbf{G}} = \overrightarrow{\mathbf{G}_r} + \overrightarrow{\mathbf{G}_\varphi}$ for a spinning G/RFg-force field.

The real situation may be more complicated: just like a point charge's $\vec{\mathbf{E}} = \overrightarrow{\mathbf{E}_r}$ propagates in r-1D with the speed of light c, a photon's $\vec{\mathbf{E}} = \overrightarrow{\mathbf{E}_\varphi}$ propagates in φ-1D may also with the speed of light c, and this propagation forced φ-1D space to "increase" its size, and then the size "increasing" of the φ-1D space is further transformed into a r-1D space expending. (Note: This is the third example of dynamic space transformation (from φ-1D to r-1D). See SunQM-6s7's section VII-c for other two dynamic space transformation: either from φ-1D to θ-1D, or from nL0 mode to nLL mode). This is the reason that a photon is always increasing its (r-1D) size (as it is propagating in x-direction), because it is actually increasing its φ-1D size. Then, plus a photon's $\overrightarrow{\mathbf{E}_\varphi}$ spins in ±φ direction alternatively (as acceleration/deceleration (see SunQM-6s2), or as ABCBA cycle (see SunQM-6s5's Fig-5), or as the effective ±m quantum number (see SunQM-6s7's Fig-5b)), this makes a photon's expending-size to show an onion-like shell structure (see SunQM-6s5's Fig-6). (Note: Also see SunQM-6s5's Appendix B for more discussion).

If the above explanation is correct, then when $\overrightarrow{\mathbf{E}_r} \to 0$, $\overrightarrow{\mathbf{E}_\varphi}$ has to go to maximum, the r-1D propagation (in light speed c, or r = ct) should be transformed into φ-1D, meaning $\overrightarrow{\mathbf{E}_\varphi}$ may spin in light speed at $2\pi r = ct$, or, $r = [c/(2\pi)]t$. This means, a spinning $\overrightarrow{\mathbf{E}_\varphi}$ may expend in r-1D in speed of $c/(2\pi)$. However, in SunQM-6s1, I had assumed that a x-directional propagating photon ball will expend in r-1D with the speed of c. If the speed c is correct, then a photon ball's r-1D expending in c will have a φ-1D propagation speed in $c*(2\pi)$, not the $c/(2\pi)$. I will leave this discrepancy to the future study. (Note: SunQM study is a global fitting process. A global fitting (initially) only fits the main things, ignores many details. If want to fit every details (initially), the global fitting will go to the wrong direction. For example, Mars was wrongly fitted as the mass accretion in {1,6//6}o orbital space during my initial Solar {N,n} structural global fitting, but then was corrected as the accretion of the residue |6,5,m> QM state (stream-like) mass in {1,5//6}o orbital space (in my next several rounds of global fitting)).

Although the analytical formula for E/RFe-force field (in the classical physics) has been characterized in Maxwell's equations, I believed that there should be an independent analytical formula for the E/RFe-force field (and also for the G/RFg-force field) in a Schrodinger equation based form (e.g., in either the Born probability form or in NBP form, see Figure 2 through Figure 4, and also see SunQM-6). For this reason, in SunQM-6s4, I worked out that not only a point charge's static electric field strength E ∝ 1/r^2, but also its potential field U ∝ 1/r, can be reconstituted directly by using the H-atom's Schrodinger equation/solution (in form of the radial Born probability density functions) in the form of {N,n//6} QM structure. This work also showed that all point-centered fields (including both the mass field, the force field, and the energy field, etc.) can be represented in the form of 3D spherical wave packet. However, I am still not absolutely sure whether this (the result in SunQM-6s4) is the ultimate analytical formula for E/RFe-force field (in {N,n} QM).

I-b. Explanation of a translating and/or spinning charge's $\vec{\mathbf{E}}$ and $\vec{\mathbf{B}}$ vector's |n,*l*,m> QM mode in the {N,n} QM field theory

The previous section was based on the vector analysis. In the current section, I do the similar analysis but based on the |n,*l*,m> QM state. (Note: From now on, the spinning $\vec{\mathbf{E}}$ vector always means the pure $\overrightarrow{\mathbf{E}_{\varphi}}$ component). In paper SunQM-6, I had re-classified the four fundamental forces to be three pair of forces: E/RFe-force, G/RFg-force, S/RFs-force, and used the combination of multiple n(s) of |n,*l*,m> QM states to describe the QM mode of $\vec{\mathbf{E}}$ vector field and $\vec{\mathbf{B}}$ vector field. Although it is more accurate, it is too complicated to handle. So, in most analysis, I no longer use the combination of n(s), but use only a single n QM state to describe the QM mode of $\vec{\mathbf{E}}$ vector and $\vec{\mathbf{B}}$ vector for the ground state (or for the excited state). Even for a single n of |n,*l*,m>, it still contains many superpositioned QM states (because for each n, *l* = 0…n-1, m = -*l*, … +*l*). For the simplest and the most characteristic description, we would like to use the two extreme ends of the series QM states for the description, that is, the nLL mode (like |2,1,1>, |4,3,3>, etc.), and the nL0 mode (like |2,1,0>, |4,3,0>, etc.).

In the {N,n} QM field theory, it is much easy to describe an E/RFe-force field by using |n,*l*,m> QM state with n=2 (as shown SunQM-6s5's Fig-1). Under this description, the original static E-force is in nL0 mode (i.e., |2,1,0>) and the original static RFe-force is in nLL mode (i.e., either |2,1,+1> or |2,1,-1>). The spin of the E/RFe-force field inversed the QM Mode of this E/RFe-force, so that the spinning E-force (meaning, the $\overrightarrow{\mathbf{E}_{\varphi}}$ part) is in nLL mode (e.g., |2,1,+1>, or |2,1,-1>, depends on the direction of the spin), and the spinning RFe-force is in nL0 mode (e.g., |2,1,0>).

Figure 2 illustrated that how a z-directional translating (with vector $\overrightarrow{\mathbf{v}_z}$) and/or spinning (with vector $\overrightarrow{\mathbf{s}_z}$) of a positive charge will affect the QM mode of its $\vec{\mathbf{E}}$ vector and $\vec{\mathbf{B}}$ vector. Here is detailed explanation (for Figure 2):

1) In the {N,n} QM field theory, I showed (from the previous SunQM-6 series papers) that for a positive charge,

1a) the original (static) $\vec{\mathbf{E}} = \overrightarrow{\mathbf{E}_r}$ vector's field should be described in nL0 mode;

1b) the +z directional translating of $\vec{\mathbf{E}} = \overrightarrow{\mathbf{E}_r}$ vector's field should also be described in nL0 mode;

1c) a spinning (with the spin vector points to +z direction) $\vec{\mathbf{E}} = \overrightarrow{\mathbf{E}_{\varphi}}$ vector should be described in nLL mode;

1d) a static $\vec{\mathbf{E}}$ vector (filed)'s orthogonal companion $\vec{\mathbf{B}}$ vector field is not only in nLL QM mode, but also in a complete RF (because a static $\vec{\mathbf{E}}$ vector is evenly distributed in all 4π directions);

1e) the +z directional translating of $\vec{\mathbf{E}}$ vector removed the RF and produced a circular $\vec{\mathbf{B}}$ vector field in xy-plane (in nLL QM mode);

1f) a spinning (with the spin vector points to +z direction) $\vec{\mathbf{E}}$ vector produces a $\vec{\mathbf{B}}$ vector field in nL0 QM mode (in pseudo +z direction, see SunQM-6), and

1g) a positive point charge that translating and/or spinning in the same +z direction is guessed to have its $\vec{\mathbf{B}}$ vector field lines spread more away from z-axis (see SunQM-6s1's Figure 4).

2) Following is the new development (at a citizen scientist level). At static ($\vec{\mathbf{v}}_z = 0$, $\vec{\mathbf{s}}_z = 0$), a positive charge's $\vec{\mathbf{E}}$ vector and $\vec{\mathbf{B}}$ vector are both (or can be best described as) at n=1 ground state, so that they both should be described by |1,0,0> QM state, and their probability density shape is in a perfect sphere (as shown by the plotting the Born probability of $|Y(0,0)|^2$ in Figure 2a and Figure 2b). The net $\vec{\mathbf{B}}$ vector = 0 (that can be explained as the fully RF). For a photon, the net $\vec{\mathbf{E}}$ (circular) vector is also zero in r-1D (if it is at |1,0,0> state). However, for a positive charge, the net $\vec{\mathbf{E}}$ vector in r-1D is not zero (even it is at |1,0,0> state. Note: see SunQM-6s5's Appendix B for detailed discussion). (Note: Alternatively, a ground state $\vec{\mathbf{E}}$ vector and $\vec{\mathbf{B}}$ vector at |1,0,0> QM state can also be described by any combination of QM states as long as it forms a spherical shaped Born probability density. Example-1: at |n,L,m> state, where n can be any single number, *l* = L = n-1, and m = -*l* … +*l*, like |4,3,m> ; Example-2: at |n,*l*,m> state, where n can be any single number, *l* is any single number between 0 and n-1, and m = -*l* … +*l*, like |4,2,m>; Example-3: at |n,*l*,m> state, where n can be any single number or combined n(s), *l* = 0 … n-1 combined, and m = -*l* … +*l*, , like |4,3,m> + |4,2,m> + |4,1,m> + |4,0,m> , etc. However, to easy the explanation of Figure 2, I ignored these alternative choices here).

3) When $\vec{\mathbf{s}}_z$ and/or $\vec{\mathbf{v}}_z$ value increases from zero to above zero, we say that the QM mode of $\vec{\mathbf{E}}$ vector and/or $\vec{\mathbf{B}}$ vector change from the ground state to the excited state, and they can be described by the n value's increasement in |n,*l*,m> QM state. The higher the $\vec{\mathbf{s}}_z$ and/or $\vec{\mathbf{v}}_z$ value, the higher the n, and the higher excited QM state (of nLL and/or nL0) that E/RFe force field will be. For example, n=1 to n=2, to n=3, or to n=4 in Figure 2 represents $\vec{\mathbf{s}}_z$ and/or $\vec{\mathbf{v}}_z$ value that changed from zero to low, to high, or to maximum. Note: here we only deal with the constant value of $\vec{\mathbf{s}}_z$ and/or $\vec{\mathbf{v}}_z$, we do not deal with acceleration or deceleration.

4) In Figure 2, I used n=4 to represent the maximum speed of $\vec{\mathbf{v}}_z$ (and/or the maximum of $\vec{\mathbf{s}}_z$). That means, at n=4, $\vec{\mathbf{v}}_z$ closes to (or even equals to) the speed of light c. (Note: Ideally, we should use $n \to \infty$ (e.g., using n = 9999 rather than n=4) to describe a positive charge's $\vec{\mathbf{E}}$ vector and $\vec{\mathbf{B}}$ vector QM mode at $\vec{\mathbf{v}}_z$ close to the speed of light. However, it is too difficult to illustrate the BP density shape of $n \to \infty$ (e.g., n = 9999) in Figure 2).

5) In Figure 2, I used Born Probability (BP, rather than non-Born probability NBP) to represent the positive charge's $\vec{\mathbf{E}}$ vector and $\vec{\mathbf{B}}$ vector, for the reason that the BP is more intuitive to show the rotation/spin process. Consequently, I have to use an arrow to show the direction of the rotation/spin, and to use the grey-patch to cover half of the BP density area (e.g., in |3,2,0>), to show that the density is uni-directional (because by default, BP density always describes the bi-directional process at the steady state).

6) As shown in the orange arrow in Figure 2a, when $\vec{\mathbf{v}}_z$ increased from zero to the light speed c, a positive charge's $\vec{\mathbf{E}}$ vector always keeps in the nL0 mode from the ground state |1,0,0> to the excited state |2,1,0>, |3,2,0>, and |4,3,0>. Following the right hand rule, its orthogonal companion $\vec{\mathbf{B}}$ vector always keeps in the nLL mode from the ground state |1,0,0> to the excited state |2,1,1>, |3,2,2>, and |4,3,3>, see the orange arrow in Figure 2b. (Note: the |1,0,0> can be treated as either the nLL mode (because $|n_{=1}, l_{=n-1=0}, m_{=n-1=0}>$), or as the nL0 mode (because $|n_{=1}, l_{=n-1=0}, m_{=0}>$)). That the $\vec{\mathbf{B}}$ vector's density shape changed from a sphere at |1,0,0> to a donut shape at |2,1,1>, and then more and more flatten donut shape at |3,2,2> and |4,3,3>, can be explained as the length contraction effect of the special relativity that caused z-dimensional compressing (by a factor of $\sqrt{1 - v^2/c^2}$, see [32]) as the $\vec{\mathbf{v}}_z$ increased from zero to the light speed c.

7) As shown in the green arrow in Figure 2a, when $\vec{\mathbf{s}}_z$ increased from zero to high speed, a positive charge's $\vec{\mathbf{E}}$ vector always keeps in the nLL mode from the ground state |1,0,0> to the excited state |2,1,1>, |3,2,2>, and |4,3,3>. Following the right hand rule, its orthogonal companion $\vec{\mathbf{B}}$ vector always keeps in the nL0 mode from the ground state |1,0,0> to the excited state |2,1,0>, |3,2,0>, and |4,3,0>, see the green arrow in Figure 2b. It is interesting to see that the spinning $\vec{\mathbf{E}}$ vector's density shape changed from a sphere at |1,0,0> to a donut shape at |2,1,1>, and then more and more flatted donut at |3,2,2> and |4,3,3>, may can also be explained as the length contraction effect of the special relativity that caused z-dimensional compressing (by a

factor of $\sqrt{1-v^2/c^2}$,) as the $\overrightarrow{\mathbf{s}_z}$ increased from zero to the maximum speed (that equivalent to the light speed c in the circular mode, see item-11 for more discussion).

8) When $\overrightarrow{\mathbf{v}_z}$ and $\overrightarrow{\mathbf{s}_z}$ both > 0, the n > 1. If the positive charge's $\overrightarrow{\mathbf{v}_z}$ value is fixed while $\overrightarrow{\mathbf{s}_z}$ value is increasing (from zero), then the $\vec{\mathbf{E}}$ vector's |n,*l*,m> QM state shifted from m = 0 to m = 1, … up to m = +*l* (see the blue arrow in Figure 2a that shifting leftward to decrease the n*l*0 component and increase the nLL component). For example, if choose n=4, then it shifted from |4,3,0> to |4,3,1>, |4,3,2>, and |4,3,3>. A more accurate description is that all four QM states, |4,3,0>, |4,3,1>, |4,3,2> and |4,3,3>, are in superposition, the QM state shift is achieved by changing the distribution probability among these four states. So, when completely shifted to |4,3,3>, the |4,3,0> component has to decrease to zero. This means, for the $\vec{\mathbf{E}}$ vector, between the $\overrightarrow{\mathbf{v}_z}$ value and the $\overrightarrow{\mathbf{s}_z}$ value, only one value can get maximum, and if one value get maximum, another one value must be zero. At the same time, the $\vec{\mathbf{B}}$ vector's |n,*l*,m> QM state shifted from m = +*l* down to m = 0 (see the blue arrow in Figure 2b that shifting leftward to decrease the nLL component and increase the n*l*0 component).

9) Similarly, when the positive charge's $\overrightarrow{\mathbf{s}_z}$ value is fixed while $\overrightarrow{\mathbf{v}_z}$ value is increasing (from zero), then the $\vec{\mathbf{E}}$ vector's |n,*l*,m> QM state shifted from m = +*l* down to m = 0 (see the pink arrow in Figure 2a that shifting rightward to decrease the nLL component and increase the n*l*0 component), while the $\vec{\mathbf{B}}$ vector's |n,*l*,m> QM state shifted from m = 0 up to m = +*l* (see the pink arrow in Figure 2b that shifting rightward to decrease the n *l*0 component and increase the nLL component). (Note: Can we have $\overrightarrow{\mathbf{v}_z}$ value and $\overrightarrow{\mathbf{s}_z}$ value both at maximum? No. According to Figure 1b, the maximum of $\overrightarrow{\mathbf{s}_z}$ value will force $\overrightarrow{\mathbf{v}_z}$ value to be zero, and vice versa).

10) To accommodate the "|nL0> Elliptical/Parabolic/Hyperbolic Orbital Transition Model", a new x'y'z'-coordinate is always set as that the translation (of the $\vec{\mathbf{E}}$ field vector) is in +x' direction (as the propagation direction of a low-f photon, see SunQM-6s2). Thus, the (old) z-directional translation equals to the (new) x'-directional translation.

11) If Figure 2 is correct, then, in theory, there might (or should) exist a maximum value for a positive charge's $\overrightarrow{\mathbf{s}_z}$ value (that equivalent to the light speed c is the maximum value for $\overrightarrow{\mathbf{v}_z}$). However, I guessed that in Figure 2a, if $|\overrightarrow{\mathbf{v}_z}| = |\overrightarrow{\mathbf{v}_{x'}}| = c$, then the final $\vec{\mathbf{E}}$ is always in |n,L,0> state with n→∞ and pointing to +z direction, no matter what the $\overrightarrow{\mathbf{s}_z} = \overrightarrow{\mathbf{s}_{x'}}$ value is (as long as $\overrightarrow{\mathbf{s}_z}$ is a physical meaningful value, means $\overrightarrow{\mathbf{s}_z} < \infty$).

12) For the $\vec{\mathbf{E}}$ vector, increasing $\overrightarrow{\mathbf{v}_z}$ to c makes it from |1,0,0> state to become |4,3,0> state, but not to the spinning |4,3,3> state, suggested that the $\vec{\mathbf{E}}$ vector is primarily in nL0 mode, so it should be a straight line vector, not a circular line vector. For the $\vec{\mathbf{B}}$ vector, increasing $\overrightarrow{\mathbf{v}_z}$ to c makes it from |1,0,0> to become |4,3,3>, suggested that the $\vec{\mathbf{B}}$ vector is primarily in nLL mode, so it should be a circular line vector, not a straight line vector.

13) When $\overrightarrow{\mathbf{v}_z}$ increasing to c, if $\vec{\mathbf{B}}$ vector's probability density shape change from a spherical |1,0,0> to a more and more flatten donut-shaped |2,1,1>, |3,2,2>, |4,3,3> is caused by the length contraction effect of the special relativity that squeezed z-dimension (see Figure 2b's orange arrow), then under the same situation, why $\vec{\mathbf{E}}$ vector's probability density shape change from a spherical |1,0,0> to |2,1,0>, |3,2,0>, |4,3,0> (see Figure 2a's orange arrow) does not show the same squeezed z-dimension effect? The answer might be that the $\vec{\mathbf{B}}$ vector's probability density shape does so because it is a circular line vector. For $\vec{\mathbf{E}}$ vector, it is a straight line vector, while $\vec{\mathbf{E}}$ field itself propagates at the speed of light c, the newly added $\overrightarrow{\mathbf{v}_z}$ = c makes the speed become twice of the c (besides this positive charge's $\vec{\mathbf{E}}$ field propagation at the +z direction at speed of c), and under the special relativity, it is still propagating at +z direction at the speed of one c, so that the $\vec{\mathbf{E}}$ vector's probability density shape apparently not show the squeezed z-dimension effect.

14) Note: Obviously, we can't use Figure 2 (both $\overrightarrow{\mathbf{v}_{z=x'}}$ and $\overrightarrow{\mathbf{s}_{z=x'}}$ in +z (= +x') direction, i.e., $\vec{\mathbf{E}}$ vector spins in xy-plane (= y'z'-plane) and translate in +z direction) to explain a photon's $\vec{\mathbf{E}}$ & $\vec{\mathbf{B}}$ oscillation (where $\overrightarrow{\mathbf{v}_{x'}}$ in +x' and $\overrightarrow{\mathbf{s}_{-y'}}$ in -y', i.e., $\vec{\mathbf{E}}$ vector spins in x'z'-plane and translate in +x' direction).

15) The above analysis may can be extended as: at steady state (i.e., $\vec{\mathbf{v}} = 0$ and $\vec{\mathbf{s}} = 0$), all primary forces (E-, G-, S-) are naturally (or initially) in nL0 mode, all orthogonal companion forces of the primary forces (RFe-, RFg-, RFs-) are naturally (or initially) in nLL mode. In other words, the nL0 mode component (i.e., the $\overrightarrow{\mathbf{E}_r}$) of the $\vec{\mathbf{E}}$ vector is in full amplitude, and nLL mode component (i.e., the $\overrightarrow{\mathbf{E}_\varphi}$) of the $\vec{\mathbf{E}}$ vector is in zero amplitude.

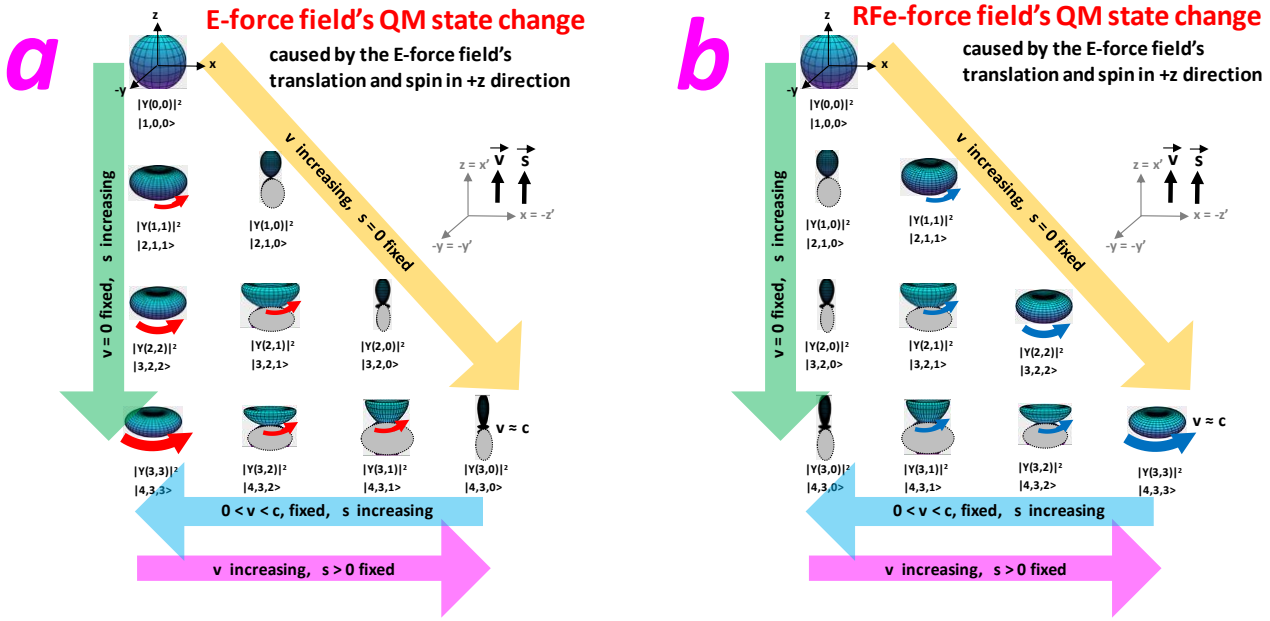

Figure 2. Explanation of a translating and/or spinning charge's $\vec{\mathbf{E}}$ and $\vec{\mathbf{B}}$ vector's |n*l*m> QM mode in the {N,n} QM field theory. All $|Y(l,m)|^2$ diagrams in this paper were plotted by using MathStudio (http://mathstud.io/) software (see SunQM-6s1's Fig-6 for detailed explanations). (Note-1: In Figure 2, the xyz-coordinate is for BP density, x'y'z'-coordinate is for the convenient of the photon to propagate in x'-direction. Note-2: I had drawn the major part of this figure in Apr. 2021. So SunQM-6s5' Fig-1 was drawn based on this figure. Note-3: in Figure 2, all nL0 mode's BP density has its half part covered by using a grey patch, to show that the BP density illustrated here should be uni-directional. Note-4: Suppose in a case we have 90% $\vec{\mathbf{E}}$ in nL0 mode, and 10% $\vec{\mathbf{E}}$ in nLL mode, Figure 2 only analyze the 10% $\vec{\mathbf{E}}$ that in nLL mode. Note-5: Once upon time I used n*l*0 instead of nL0. Now I mostly use nL0 because I try to simplified the QM state description by using a single n (and a single *l*) rather than a combination of them).

Figure 3 illustrated that how a positive charge that spinning in -y' direction (with vector $\overrightarrow{\mathbf{s}_{-y'}}$) and translating in +x' direction (with vector $\overrightarrow{\mathbf{v}_{x'}}$) will affect the QM mode of $\vec{\mathbf{E}}$ vector and $\vec{\mathbf{B}}$ vector. (Note: Again, the x'y'z' coordinate was chosen to fit to the "|nL0> Elliptical/Parabolic/Hyperbolic Orbital Transition Model" in which the $\vec{\mathbf{E}}$ vector is always spinning in x'z' plane and the newborn photon is always emitted in +x' direction). I want to show it here because it can directly explain the oscillation of $\vec{\mathbf{E}}$ and $\vec{\mathbf{B}}$ vectors in the 1D transverse electromagnetic wave (see SunQM-6s4's Fig-4). Here is detailed explanation (for Figure 3):

1) Figure 3a showed a $\vec{\mathbf{E}}$ vector's probability density when increasing its spin speed $\overrightarrow{\mathbf{s}_{-y'}}$ from n=1 to 2, 3, and 4, with the zero translation $\vec{\mathbf{v}} = 0$.

2) Figure 3b: after added (an x'-directional velocity) $\overrightarrow{\mathbf{v}_{x'}}$ = c to Figure 3a, the same $\vec{\mathbf{E}}$ vector's probability densities changed their QM states (or the QM modes, or the probability density shapes) and became Figure 3b. Because $\overrightarrow{\mathbf{v}_{x'}}$ = c compressed the x' dimension (or x' dynamic space) to nearly zero, so that a x'z'-2D space is degenerated to be a z'-1D space. Thus, the $\vec{\mathbf{E}}$ vector that was spinning in in x'z'-plane (shown in Figure 3a) now become oscillating along z' axis (shown in Figure 3b). For example, the |2,1,1> QM spinning mode now is squeezed to |2,1,0> QM oscillation mode with the $\vec{\mathbf{E}}$ vector oscillated points to +z' and then to -z' directions. Notice that this correlated well to 1D transverse electromagnetic wave's $\vec{\mathbf{E}}$ vector that always oscillating in ±z direction (see SunQM-6s5's Fig-4a). (Note: because vectors $\overrightarrow{\mathbf{v}_{x'}}$ = c and $\overrightarrow{\mathbf{s}_{-y'}}$ = max are not in the same direction, so both vectors can be maximum values. It is not like that if $\overrightarrow{\mathbf{v}_{x'}}$ = c, then it has to be $\overrightarrow{\mathbf{s}_{x'}}$ = 0).

3) Figure 3c: for the Figure 3a's spinning $\vec{\mathbf{E}}$ vector produced $\vec{\mathbf{B}}$ vector (refer to Figure 2b's green arrow, although the x'y'z'-coordinate oriented differently), the adding of $\overrightarrow{\mathbf{v}_{x'}}$ = c caused x'-dimensional compression has little effect on the $\vec{\mathbf{B}}$ vector's probability density shape (of |2,1,0>, |3,2,0>, and |4,3,0>), because it is mainly distributed on the y' axis, so that the $\vec{\mathbf{B}}$ vector's probability density shape still can be represented by |2,1,0>, |3,2,0>, and |4,3,0> after $\overrightarrow{\mathbf{v}_{x'}}$ = c (as shown in Figure 3c).

4) After we carefully align the time phase of t_1 that correlates to the $\vec{\mathbf{E}}$ vector in Figure 3a start to spin from +z' to -x' (e.g., in |2,1,1> mode), it will correlate to the same $\vec{\mathbf{E}}$ vector (also use |2,1,1> mode) that points to +z' and starts to oscillate to -z' (in Figure 3b, the yellow circled one), and also correlate to the companion $\vec{\mathbf{B}}$ vector (that must be in |2,1,0> mode) that points to -y' and starts to oscillate to +y' (in Figure 3c, also the yellow circled one). Finally, we find that they correlate well to 1D transverse electromagnetic wave at t_1 time (see SunQM-6s5's Fig-4a) where its $\vec{\mathbf{E}}$ vector pointing to +z direction and starts to oscillate to -z direction, and its $\vec{\mathbf{B}}$ vector pointing to -y direction and starts to oscillate to +y direction, (that is, it matches the right-hand rule of the unit-vector cross-production of $\frac{\vec{\mathbf{E}}}{|\vec{\mathbf{E}}|} \times \frac{\vec{\mathbf{B}}}{|\vec{\mathbf{B}}|} = \frac{\vec{\mathbf{v}}}{|\vec{\mathbf{v}}|}$, see [33] ~ [34]).

5) Because the {N,n} QM field theory for the photon was developed in a completely different way than that of the 1D transverse electromagnetic wave, the correct correlation of $\vec{\mathbf{E}} \times \vec{\mathbf{B}}$ vectors between QM mode description (see Figure 3's two yellow circles) and 1D transverse electromagnetic wave at t_1 time does provide some special meanings for the correctness and the self-consistency of the {N,n} QM field theory:

5a) It means that the photon's |2,1,m> QM state description and ABCBA cycle description (see SunQM-6s5's section I) should be correct enough to make the whole description self-consistent;

5b) It means that the "|nL0> Elliptical/Parabolic/Hyperbolic Orbital Transition Model" should be (roughly) correct; and from it, the hypothesis of the low-f photon (i.e., the sub-Hz photon) should be (roughly) correct; also from it, a x'-direction propagating photon's $\vec{\mathbf{E}}$ vector should be spinning in x'z'-2D plane originally (rather than oscillating in z-1D);

5c) The special relativity should be (roughly) correct, because after applied it for a $\overrightarrow{\mathbf{v}_{x'}}$ = c photon, its x'z'-2D spinning $\vec{\mathbf{E}}$ vector become z'-1D oscillation, and matches the 1D transverse electromagnetic wave description;

5d) The classical physics' (or the classical electrodynamics') 1D transverse electromagnetic wave (i.e., $\frac{\vec{\mathbf{E}}}{|\vec{\mathbf{E}}|} \times \frac{\vec{\mathbf{B}}}{|\vec{\mathbf{B}}|} = \frac{\vec{\mathbf{v}}}{|\vec{\mathbf{v}}|}$) description should be (roughly) correct, because it matches the {N,n} QM field theory's photon description (as shown in Figure 3's two yellow circles);

5e) Although the text book said that "Maxwell's equations do satisfy relativity" [35], as a citizen scientist, my math level is too low to understand the mathematical proof (see wiki "Maxwell's equations" at section of "Relativistic formulations"). Now the result of my own work, (that the {N,n} QM field theory derived propagating photon's $\vec{\mathbf{E}}$ and $\vec{\mathbf{B}}$ vectors (see SunQM-6s5's Fig-5), after applying the special relativity (see Figure 3's two yellow circles), does match the Maxwell's equations derived 1D transverse electromagnetic wave (that $\vec{\mathbf{E}}$ and $\vec{\mathbf{B}}$ vectors oscillating in phase with each other and both transverse to the propagation, see SunQM-6s5's Fig-4a)), does make me to believe that "Maxwell's equations do satisfy relativity".

5f) In {N,n} QM field theory, the wave front of a photon's 3D wave packet may travels in 2 folds of light speed c (that may violate a rule in the Modern physics that c is the maximum speed); If we use the Lorentz-transformation to limit the wave front to be one c (see SunQM-6s5's Fig-8c), then we may cannot use the wave front's interference to explain the double-slit experiment (see SunQM-6s1's section III-d), because the photon's core must have speed of c. My current explanation for this

is, the wave front of a photon's spherical 3D wave packet does propagate faster than c, although as an outside observer, we are not able to see it. Constrained by the Lorentz-transformation, we always see the dynamic space of Δx' for the wave-front (from c×t to 2c×t) is compressed to zero. Nevertheless, this is the first round "Global fitting" to design the {N,n} QM field theory. We will need to do more iterations of the "Global fitting" to fix this if it becomes a problem.

6) In SunQM-6's section I-d, I mentioned that "*the nLL (with m = max) QM state force field and nl0 (with m = 0) QM state force field are topologically inter-changeable*". There I had showed the first example: when $\vec{\mathbf{v}}$ changed from a straight line motion to a circular motion, a positive charge's nL0 mode $\vec{\mathbf{E}}$ vector will change to nLL mode, and its orthogonal companion $\vec{\mathbf{B}}$ vector will change from nLL mode to nL0 mode. Now we have a second example for this kind of topological change: when $\vec{\mathbf{v}}_{x'}$ changed from zero to the speed of light, a spinning positive charge's nLL mode $\vec{\mathbf{E}}$ vector (see Figure 3a, with $\vec{\mathbf{s}}_{-y'} > 0$) will change to nL0 mode (see Figure 3b).

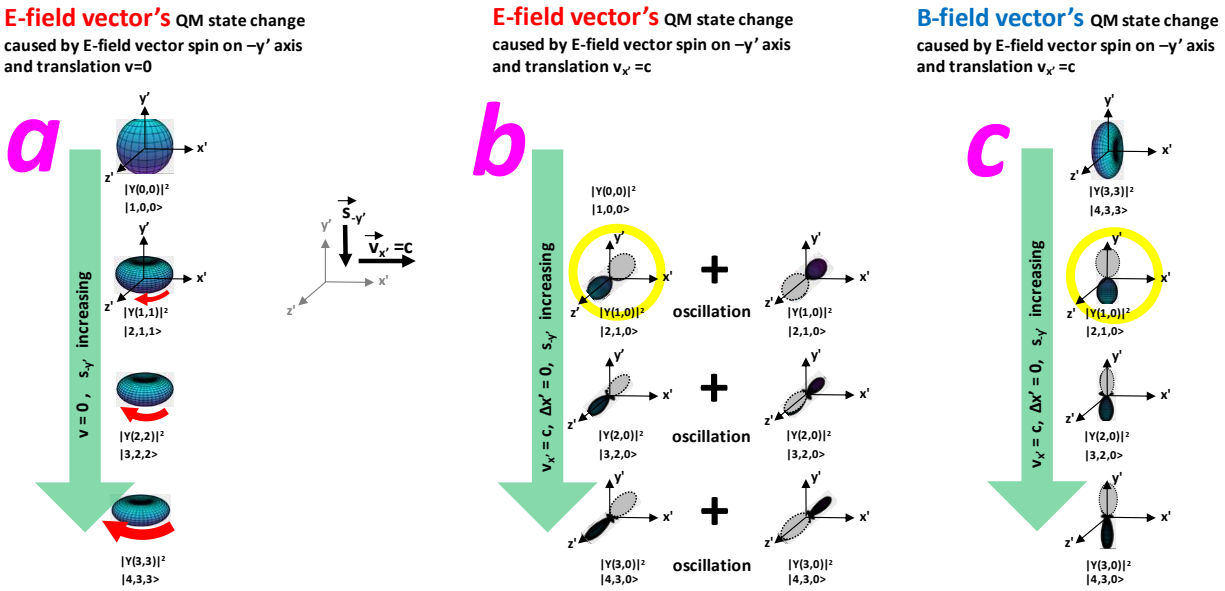

Figure 3. To illustrate that how a positive charge (that spinning in -y' direction $\overrightarrow{\mathbf{s}_{-y'}}$ and translating in +x' direction $\overrightarrow{\mathbf{v}_{x'}}$) will affect the QM mode of $\vec{\mathbf{E}}$ vector and $\vec{\mathbf{B}}$ vector. Note: in Figure 3, all nL0 mode's BP density has its half part covered by using a grey patch, to show that the BP density illustrated here should be uni-directional. Note: in Figure 3b, the |2,1,0>, |3,2,0>, and |4,3,0> density are all along z' axis. Note: The red arrows (in Figure 3a) showed the $\vec{\mathbf{E}}$ vector's spin in x'z'-2D plane from +z' to –x' (to fit to the elliptical orbital model), and the $\vec{\mathbf{B}}$ vector density pointed in the -y' direction consequently (in Figure 3c).

As I mentioned before (see SunQM-7's Appendix G), the only necessity of the existence of the citizen scientists is to broaden the foundation of existing physics (or science). The citizen scientists do so by sprouting out many new and wild (or diversified) ideas that are completely deviated from the current main stream theory. Although almost all of these wild ideas died out very soon (because they are either too far from the correct or they are the repeated ideas), a few sprouts (like Einstein's special relativity in 1905) did grown-up to be a new direction for the physics. This is exactly like Darwin's theory of natural selection. As a citizen scientist, one of my hopes is to design a new {N,n} QM field theory that is largely deviated from the Modern Quantum Field theory (like QED, QCD, String Theory, etc.). However, the result of the new {N,n} QM field theory should match to the result of the existing (mainstream) classical/quantum theory as much as possible, or

whenever it is possible, (besides it should match the experimental data). I am really glad that for a propagating photon's $\vec{\mathbf{E}}$ and $\vec{\mathbf{B}}$ vector description, the new {N,n} QM field theory does match to the classical theory (i.e., Maxwell's equations) and the Modern Quantum Field theory (see [36], although it is beyond my math level). In other words, the newly developed {N,n} QM field theory does broaden the foundation of the Maxwell's equations, the relativity theory, and the Modern Quantum Field theory, (at least and only for the part of a propagating photon's $\vec{\mathbf{E}} \times \vec{\mathbf{B}}$ vector description). The reason why I want to mention this is that in several cases, the new {N,n} QM field theory's results did un-match to the existing (mainstream) classical/quantum theory's results. For example, the {N,n} QM field theory re-classified the traditional quantum field theory's four fundamental forces into three pairs (see SunQM-6); Although the {N,n} QM field theory had a surprising good match with the Modern Quantum Field theory's Standard Model of particles in the part of the down-quark's 1st, 2nd, 3rd generations (see SunQM-5s2's Table 2), it does have some significant discrepancies (also see SunQM-5s2's Table 2, although these discrepancies do not seem to make these two theories mutual exclusive. I hope that both theories can be successful, to become another Thermodynamic vs Statistic Mechanics, or another Bohr-QM vs Schrodinger-QM); Even more surprisingly, the {N,n} QM field theory is mutually exclusive with the current mainstream theory of the expanding universe (and Big Bang, and dark energy, see SunQM-7's section V).

II. Two pairs of E/RFe-force: the RFe-RFe interaction (limited the discussion to the spin-spin interaction between the two electrons in the same electron orbital)

II-a. The RFe-RFe spin-spin interaction based on the classical physics

From the knowledge of classical physics, if we put many small magnetic bars around a big magnetic bar, we know how those small magnetic bars will be oriented (shown in Figure 4c). Also if we forced all these small magnetic bars in certain direction, we know what the force direction and the force strength that these small magnetic bars will be exerted (shown in Figure 4a and b). This is exactly how the two pairs of E/RFe-force (the "master" one the "subordinate" one) will interact with each other through the RFe-RFe interaction (or through the spin-spin interaction). (Note: Can we use n=2, 3, 4, to describe spin-spin interaction's strength? I will try it in the future).

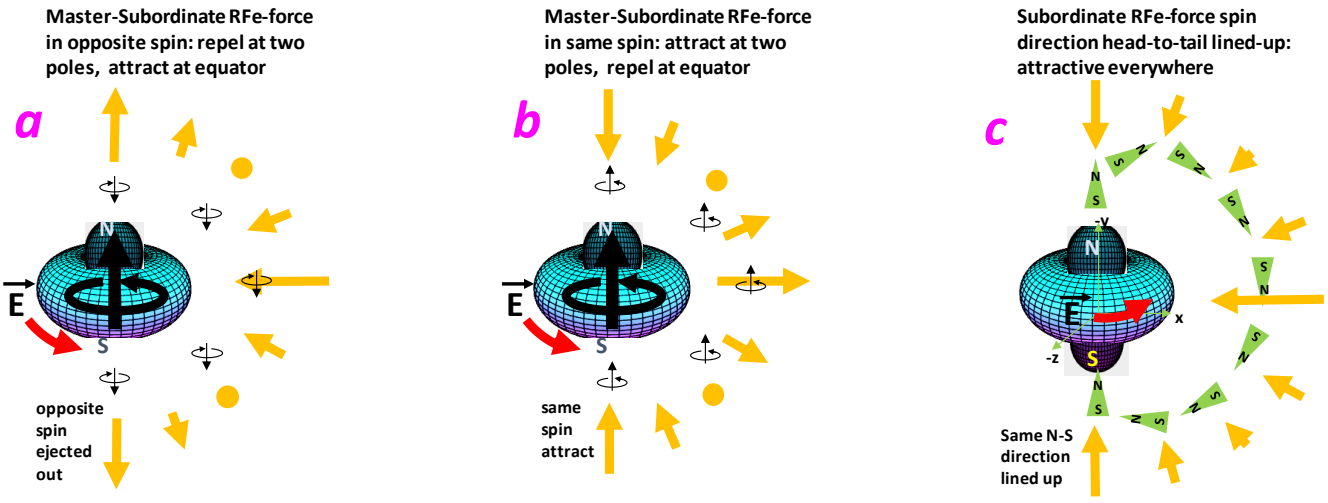

Figure 4. Illustration of how the two pairs of E/RFe-force (the master one the subordinate one) will interact with each other through the pure RFe-RFe interaction (or through the spin-spin interaction). The orange arrow: its direction represents the

spin-spin interaction force's direction, and its length represents the spin-spin interaction force's strength. (Note: the force strength in Figure 4 is a pure guess).

II-b. Two or more (same n shell or same *l* sub-shell) electrons' parallel spin configuration

(Note: From the section I-a, we see that the two charges' spin-spin interaction is really the "inversed RFe"-"inversed RFe" interaction. However, in {N,n} QM field theory, for simplicity, we usually (inaccurately) call it "**RFe-RFe interaction**").

Although in both classical physics and the Modern QM, there are many good descriptions for the spin-spin interaction, in the {N,n} QM field theory, this part is still very lag behind. In the {N,n} QM field theory, this topic should cover the general RFe-RFe interaction. However, it is a too big and too complicated task for me now. In this section, I limited our discussion on the RFe-RFe interaction only to the two (or more) same orbital electrons' spin-spin interaction. Again, for simplicity, here we only use nLL mode and nL0 mode with n=2 for the description

Although a single electron $\vec{\mathbf{E}}$ vector's spin should be described with nLL QM mode, its spin vector $\vec{\mathbf{s}}$ should be described with nL0 mode (e.g., |2,1,0> state). In BP density, we can use the un-covered top-half-part of the |2,1,0> state to represent the spin ↑ (see SunQM-6s5's Fig-1j), and use the un-covered bottom-half-part to represent the spin ↓ (see SunQM-6s5's Fig-1q). In NBP density, we can directly use the top-positive wave function of |Y(1,0)|^2 to represent the spin ↑ (see SunQM-6s5's Fig-1m), and use the bottom-positive wave function of |Y(1,0)|^2 to represent the spin ↓ (see SunQM-6s5's Fig-1t).

According to the text book, at the ground state, the outmost shell's electron configuration (in an atom) is determined by the combination of Aufbau's rule, Hund's rule, and Pauli exclusion principle, to have the lowest total binding energy. Here I showed one example (that may have some common characters as that in the RFg-force's spin-spin interaction): According to wiki "Orbital hybridization", "*For a tetrahedrally coordinated carbon (e.g., methane CH_4), … Carbon's ground state configuration is* $1s^2 2s^2 2p^2$ " with the spin configuration shown in Figure 5a. "*The carbon atom can also bond to four hydrogen atoms by an excitation … of an electron from the doubly occupied 2s orbital to the empty 2p orbital, producing four singly occupied orbitals*" (see Figure 5b). Under the sp^3 hybridization, carbon's all four n = 2 orbital electrons (now they are fully equivalent with each other due to the hybridization) take the same spin direction ↑↑ (see Figure 5c). Under either the sp^2 hybridization or sp hybridization, these four n = 2 orbital electrons still take the same spin direction ↑↑ (see Figure 5c and Figure 5d).

In the {N,n} QM field theory, we may name the ↑↑ oriented and paired spin-spin attractive interaction as the "**parallel nL0-to-nL0**", and the ↑↓ oriented and paired spin-spin interaction as the "**antiparallel nL0-to-nL0**".

In SunQM-6s7, I had hypothesized that the spin of both the electron and the nucleon (in an atom) may originate from the face-to-face tidal-locked binary circular orbital rotation between them. This hypothesis also perfectly fits to the new "proton-electron mirror-coupled orbit" model (in SunQM-6s6). The result of Bohr-QM formula $L_{n,orbit} = mv_n r_n = n\hbar$ may directly support this hypothesis. Besides the spin-spin interaction between the electron and the proton in an H-atom (shown in SunQM-6s7's Fig-5a), I also showed the possible spin-spin interaction between the two electrons in the same n=1 shell in an He-atom (in SunQM-6s7's Fig-5c); and the possible spin-spin interaction configuration between the two electrons and four nucleons in an He-atom (in SunQM-6s7's Fig-5d). More research work need to be done to further develop these ideas (before it can be a general method). (Note: In SunQM-6s7's Fig-2, I showed one way to present a snapshot of the paired spin up/down electrons (that is in complete RF) in one n shell by using the spherical harmonic function Y(*l',m'*). However, this method seems cannot be used to explain the spin-spin interaction so far).

For carbon's four electrons (in the n=2 outmost shell) in CH_4 molecule, they always repel with each other (due to the Coulombic force). With the chance to pair to the electrons from four H-atoms, these four n=2 electrons want to stay away from each other the farthest. By taking the ↑↑↑↑ spin configuration (inn Figure 5c), they have the strongest repulsive force between them (because now both the Coulombic force and the Pauli exclusion principle force are added rather than subtracted). This provides the longest distance between the carbon nucleus and the hydrogen nucleus in the C-H σ-bond (to

minimize the four n=2 electrons' Coulombic repulsion in C-atom's θφ-2D space), and thus make the total binding energy of the CH_4 molecule the lowest (or, the global energy minimization). This may be exactly the same as that in a galaxy's arm, the neighboring star's ↑↑↑↑ parallel spin configuration provided the extra attractive force so that the total binding energy of the whole arm (as a virtual chain-like entity) become the lowest (see section IV).

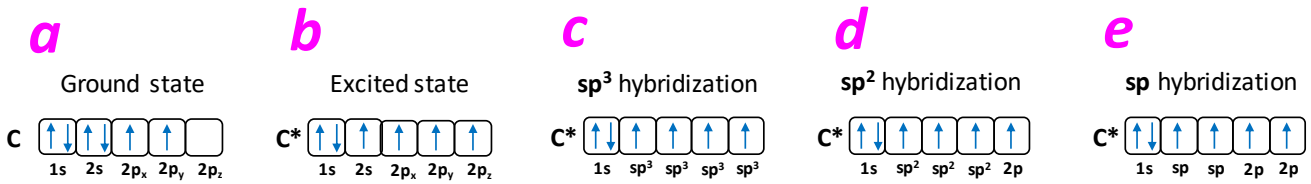

Figure 5. Illustration of a carbon atom's n=2 electron configuration and spin configuration at different QM state. (Note: Figures were copied and modified mainly from wiki "Orbital hybridization").

III. One single pair of G/RFg-force: More exploration on a translating and/or spinning celestial body's |n,*l*,m> mode in the {N,n} QM field theory.

III-a. For a spinning G/RFg-force field, the vector decomposition of $\vec{\mathbf{G}} = \overrightarrow{\mathbf{G}_r} + \overrightarrow{\mathbf{G}_\varphi}$ also gives $\overrightarrow{\mathbf{G}_r}$ correlating to nL0 mode, and $\overrightarrow{\mathbf{G}_\varphi}$ correlating to nLL mode

Again, we name the (non-spinning) G-force (or G-force-field) as the "**$\vec{\mathbf{G}}$ vector**", and name its orthogonal companion RFg-force (or RFg-force-field) as the "**$\overrightarrow{\mathbf{RFg}}$ vector**". For the spinning $\vec{\mathbf{G}}$ vector (where $\vec{\mathbf{G}} = \overrightarrow{\mathbf{G}_r} + \overrightarrow{\mathbf{G}_\varphi}$), we name the pure sinning part (i.e., $\overrightarrow{\mathbf{G}_\varphi}$) as the "**inversed $\vec{\mathbf{G}}$ vector**", and name the inversed $\vec{\mathbf{G}}$ vector produced $\overrightarrow{\mathbf{RFg}}$ vector as the "**inversed $\overrightarrow{\mathbf{RFg}}$ vector**". The vector decomposition of $\vec{G} = \overrightarrow{G_r} + \overrightarrow{G_\varphi}$ for a spinning G/RFg-force field (in Figure 1c and Figure 1d) showed the same result for a spinning E/RFe-force field (in Figure 1a and Figure 1b)). (Note: However, according to Figure 1d, on the surface of a black hole where the spinning makes the $\overrightarrow{G_\varphi}$ to maximum, will it make $\overrightarrow{G_r} \to 0$? It will be discussed in SunQM-7s1).

III-b. Explanation of a translating and/or spinning celestial body's $\vec{\mathbf{G}}$ vector and $\overrightarrow{\mathbf{RFg}}$ vector in the {N,n} QM field theory with |n,l,m> QM mode

In the {N,n} QM field theory, the G/RFg-force is described in the same way as that for E/RFe-force:

1) Like that of E/RFe-force field, the G/RFg-force field may can also be described by the Schrodinger equation/solution, i.e., the QM state of |n,*l*,m>, in the form of either the Born probability 3D density diagram, or the non-Born probability (NBP) 3D density diagram.

2) Again, in {N,n} QM field theory, it is impractical to use the combination of multiple n(s) of |n,*l*,m> QM states (see SunQM-6's Table 2 and eq-1) to describe the QM mode of $\vec{\mathbf{G}}$ vector and $\overrightarrow{\mathbf{RFg}}$ vector. So now we use only a single n QM state to describe the QM mode of $\vec{\mathbf{G}}$ vector (i.e., G-force) and $\overrightarrow{\mathbf{RFg}}$ vector (i.e., RFg-force). As usual, for the $\vec{\mathbf{G}}$ vector's and $\overrightarrow{\mathbf{RFg}}$ vector's translational speed, the spin-speed, or the RFg-RFg interaction intensity, we use the low n to describe the ground state (means the zero speed, or zero intensity), and use the high n to describe the excited state (means the high speed, or high intensity).

3) Again, even for a single n of |n,*l*,m>, it still contains many superpositioned QM states (because for each n that greater than 2, *l* = 0…n-1, m = -*l*, … +*l*). For the simplest and the most characteristic description, we would like to use the two ends of the series QM states for the description, that is, the **nLL mode**, and the **nL0 mode**. For the simplest, I quite often use n=2, that is, the nL0 mode |2,1,0> and the nLL mode |2,1,±1> for the description.
4) Again, although a single celestial body's spinning motion should be described with nLL QM mode, its spin vector $\vec{\mathbf{s}}$ should be described with nL0 mode (e.g., |2,1,0> state). In BP density, we can use the un-covered top-half-part of the |2,1,0> state to represent the spin ↑ (see SunQM-6s5's Fig-1j), and use the un-covered bottom-half-part to represent the spin ↓ (see SunQM-6s5's Fig-1q). In NBP density, we can directly use the top-positive wave function of |Y(1,0)|^2 to represent the spin ↑ (see SunQM-6s5's Fig-1m), and use the bottom-positive wave function of |Y(1,0)|^2 to represent the spin ↓ (see SunQM-6s5's Fig-1t).
5) Following figures (that used to describe the character and behavior of E/RFe-force) are also can be used to describe the character and behavior of G/RFg-force: Figure 2, Figure 3, Figure 4 in the current paper, and SunQM-6's Fig-1, Fig-3, Fig-4, Fig-5, Fig-7, and Fig-8.
6) Thus, Figure 2 should can be directly used to describe G/RFg-force's |n,*l*,m> QM state for a Sun (or a planet). Because Sun's translational speed and/or spin speed is small, n=2 QM state could be a good description. However, to describe the |n,*l*,m> QM state of a fast-spin neutron star's spin vector $\vec{\mathbf{s}}$, or a celestial body that head-to-head hit into a black hole, we may need the use high n number for the description. Also, based on Figure 2, we see that for the same pre-Sun ball, a disk-lyzation (or, disk-forming) process is a nLL effect evolution process that from the low n (or the base n) to high n', and this is very similar as the Y*lm* cycle process that also from the low n (or the base n) to high n', or a photon propagation process that also from the low n to high n.
7) Spinning of a G-force (or a pair of G/RFg-force) will produce a reference-spin-frame (like a Sun-Spin-Frame, or "**SunSpnFrm**" in SunQM-3s1). If there is < 1% mass occupancy in this reference-spin-frame, then,
7a) the nLL QM-force (that the SunSpnFrm produced) intended to disk-lyze (or, disk-forming) all matter in a spherical shell (by degenerating (m = -*l*, ... +*l*) to m = +*l*), and also to segregate a disk into several rings (by degenerating (*l* = 0, ... (n-1)) to *l* = n-1), and then also to accrete all matter in a single orbital ring into a planet (by degenerating multiple peaks in a circular 1D wave function into 1 peak, $e^{im\varphi} = \left(e^{i\varphi/2}\right)^{2m}$, see SunQM-4s1's eq-26 and Fig-6);
7b) the nL0 QM-force (that the SunSpnFrm produced) intended to slow down the kinetics for the collapsing (of the ~99% mass) at the two pole side, so that it appeared to have the bipolar outflow during the collapsing process.
7c) However, if there is ~ 100% mass occupancy in this reference-spin-frame, then the nLL QM-force (that the Sun's SpnFrm produced or the planet's SpnFrm produced) intended to flatten the spherical ball of the Sun's body (or the planet's body) by shifting the mass distribution from (m = -*l*, ... +*l*) to more in m = +*l*),), and may also intended to segregate a continues r-distribution of the mass density into several stepped r-distribution (e.g., planetary differentiation, Sun's radiation/convective zone formation).

III-c. A complete description for the nLL QM-force

From the first order spin-perturbation calculation (in SunQM-3s1), I showed that the spin of a star (and/or a particle) will produce the nLL QM effect. This nLL QM-effect will disk-lyze (or disk-forming) the mass distribution at outside the Sun (or a pre-Sun ball) to make a disk shape for the Solar system. The same nLL QM-effect will flatten the planet Saturn's body from a perfect spherical shape. Because the nLL QM-effect works like a pseudo force to push the matter at the two pole sides (of one spherical n shell) to the equator (or from θ = 0 and π to θ = π/2), we named it as the **nLL QM-force**. Here is a complete description of the "nLL QM-force": it is a pseudo force that only exist in a **RefSpnFrm** (**reference-spin- frame**, just like that either the centrifugal force or the Coriolis force is a pseudo force, and they also only exist in a RefSpnFrm). It contains a θ-1D component force that forces n state mass from two pole (and high latitude) to the equator (or, it degenerates m = -*l*, … +*l* to be m = +*l*, i.e., the pseudo force that forces a ball-shape structure into a disk-shape structure); it also contains a Δr-1D component force that forces n state mass distribution from either $r < r_n$ or $r > r_n$ to exact $r = r_n$ for each of n shell orbit

(i.e., the pseudo force that dissect a disk into several rings, or, degenerates (l = 0, ... (n-1)) to l = n-1). (Note: Usually when we mentioned "nLL QM-force", we (almost) always refer to its θ-1D force that forcing a ball into a disk, we rarely concern its Δr-1D component force that forcing a disk into a series of rings). However, this nLL QM-effect is only noticeable or obvious in the G/RFg-froce system in the macro-world, it seems that there is no noticeable nLL QM-effect reported in a E/RFe-force field system in the micro-world (e.g., in an atom), probably due the that in the micro world, the RF effect (or the "RF-force") is much stronger than the nLL QM-force.

In SunQM-3s10's Fig-8, I showed that for our Sun, the stop-line of the nLL-force (θ-1D force) is guessed at {4,1//6}, the stop-line of the bound-state G-force (r-1D force) is guessed at {5,1//6}, the stop-line of the unbound-state G-force (r-1D force) is guessed at {6,1//6}. Based on that, I believed that the nLL QM-force's sub-force of disk-lyzing is a short force in comparison with its primary G-force (r-1D force). For the nLL QM-force's sub-force that dissecting a disk into rings, because it only act either within a super-shell of ΔN = 1, or within a shell of Δn = 1, it must also be a short force in comparison with its primary G-force (r-1D force).

Because the nLL QM-force is mainly in θ-1D dimension, it belongs to one special kind of RF-force that exists naturally in θφ-2D dimension (rather than the primary force that naturally exists in r-1D dimension). In general, based on the text book knowledge that the Weak-force (i.e., RGs-force) is a short force in comparison with the Strong-force (i.e., S-force, see wiki "Strong interaction"), I guessed that all RF-forces (including RFe-force, RFg-force, and RFs-forces) could be the relative short-distance force in comparison with their primary (r-1D-only) forces (i.e., E-force, G-force, and S-force).

IV. Two pairs of G/RFg-force: More exploration on the RFg-RFg interaction (in terms of spin-spin interaction)

(Note: Same as E/RFe-force's spin-spin interaction, the two celestial bodies' spin-spin interaction is really the "inversed RFg"-"inversed RFg" interaction. However, in {N,n} QM field theory, for simplicity, we usually (inaccurately) call it "**RFg-RFg interaction**").

IV-a. The RFg-RFg (spin-spin) interaction analysis that based on the result of the RFe-RFe (spin-spin) interaction

In SunQM-3s1, I mentioned that in a big (or the "master") celestial body's spin produced RefSpnFrm, most small (or the "subordinate") celestial bodies will stay in (or moved to) the (lowest energy) nLL QM state at the equator plane (of this RefSpnFrm), and this is caused by the nLL QM-force that from the spinning of the primary G-force. According to Figure 4 (that is for RFe-RFe spin-spin interaction), I generated Figure 6 that is for RFg-RFg spin-spin interaction (with the hypothesis that the parallel RFg-RFg spin-spin interaction is attractive). I guessed that in the "master" celestial body's RefSpnFrm, for the "subordinate" celestial body, if it has the anti-parallel spin, then it will be repelled by the master at any position in the RefSpnFrm (probably maximum at the equator plane, through the antiparallel spin-spin interaction, see Figure 6a); if it has the parallel spin, then it will be attracted by the master at any position in the RefSpnFrm (probably maximum at the equator plane, through the parallel spin-spin interaction, see Figure 6b); and (in comparison with that of Figure 4c), Figure 6c has not much meaning. Of cause, we need do experiment to determine whether Figure 6 is correct, and if correct, what is the strength for these force vectors. See Appendix A for more discussions.

Note: Figure 6b matches with the hypothesis in SunQM-6s7's section VII-a: the face-to-face tidal-locked state is the Eigen state (or the global energy minimum state) of a binary orbital movement. (Note: the face-to-face tidal-locked binary orbital motion will produce a parallel spin-spin interaction physically).

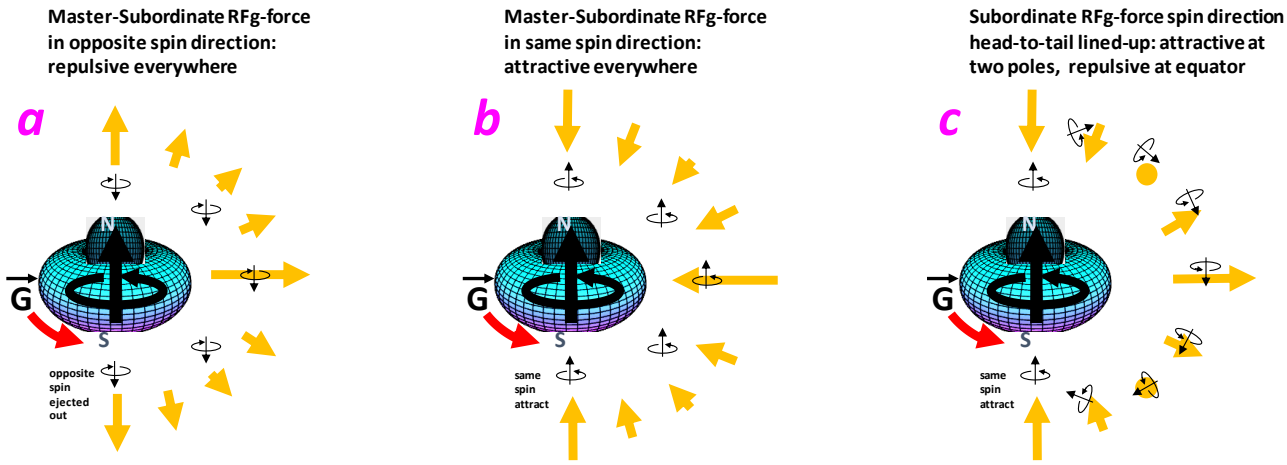

Figure 6. Illustration of how the two pairs of G/RFg-force (the "master" one and the "subordinate" one) will interact with each other through the pure RFg-RFg interaction (or through the spin-spin interaction). The orange arrow: its direction represents the spin-spin interaction force's direction, and its length represents the spin-spin interaction force's strength. (Note: the force strength in Figure 6 is a pure guess).

IV-b. Examples of RFg-RFg interaction in form of the parallel spin-spin attractive interaction

For the interaction between the binary celestial bodies, the master celestial body's Schrodinger equation naturally already included the G-force to G-force (i.e., the master's $\overrightarrow{\mathbf{G}_r}$ to the subordinate's $\overrightarrow{\mathbf{G}_r}$, see Figure 7) interaction with the subordinate celestial body (e.g., the Sun interact with the Earth as shown in in SunQM-3s11's eq-49, or similarly, the Schrodinger equation of H-atom describes the E-force to E-force interaction between the "master" proton and the "subordinate" electron, through the potential function in the Hamiltonian). In SunQM-6s7, I hypothesized that the "face-to-face tidal-locked binary circular orbital rotation between them" is the possible spin origin of either the electron and nucleon in the atom, or the star and planet in a solar system. The preliminary work in SunQM-6s7 suggested that the spin information of either the electron and nucleon in an atom, or the star and planet in a solar system, may have also already included in their Schrodinger equation/solution (or in the Bohr-QM formula in SunQM-6s7's eq-27, and in SunQM-6s7's eq-28). However, we still don't know how to extract out the quantitative result of the spin dynamics (i.e., the direction, the strength, etc., of the parallel nL0-to-nL0 attraction, or $\overrightarrow{\mathbf{G}_\varphi}$ to $\overrightarrow{\mathbf{G}_\varphi}$ interaction) directly from the Schrodinger equation/solution. Thus, there is still a long way to go before we can get it.

In the section III-c, the RFg-RFg interaction was guessed as a secondary (or a weaker) force and has a shorter action distance (in comparison with the primary G-force to G-force interaction, just like the Magnetic-force relative to the Electric-force, or the Weak-force relative to the Strong-force). Figure 6b showed that for those subordinate objects that orbiting the master celestial body at the nLL plane, the parallel spin-spin attractive interaction (as the RFg-RFg interaction) will strengthen the attractive force (i.e., the primary G-force attraction plus the RFg-RFg attraction). The hypothesis that "the spin of both the electron and the nucleon (in an H-atom) may originate from the face-to-face tidal-locked binary circular orbital rotation between them" (in SunQM-6s7) will automatically causes the spin of proton and electron in the same direction physically (i.e., physically ↑↑, although this means the electric spin is in ↑↓ due to their opposite charges). In SunQM-6s7's section-VIII, I also showed that the {N,n} QM caused pre-Sun ball collapse, disk-lyzation, and accretion will make all planets spin in the same direction as that of the Sun. For this reason, I guessed that most stars (and other objects) in a galaxy's disk (i.e., in the equator plane of a Super-Massive-Black-Hole (**SMBH**)'s RefSpnFrm) have their spins in parallel (or near-parallel) with the spin of the SMBH (see section V below). This is also the reason why our Moon is located at the equator plane of Earth's RefSpnFrm, and have the spin in parallel with that of the Earth (see the Example-2 below). This is also the

reason why all moons are located at the equator plane of Uranus's RefSpnFrm (notice that Uranus's RefSpnFrm is nearly 90° deviated from the Sun's RefSpnFrm), and I guessed that the spins of most (if not all) of these moons are in parallel with that of the Uranus. This is also the reason why a companion star should be located at the equator plane of the master black hole's RefSpnFrm, and have the spin in parallel with that of the black hole (see the Example-3 below). Following are the three examples of RFg-RFg interaction in forms of the parallel spin-spin's attractive interaction.

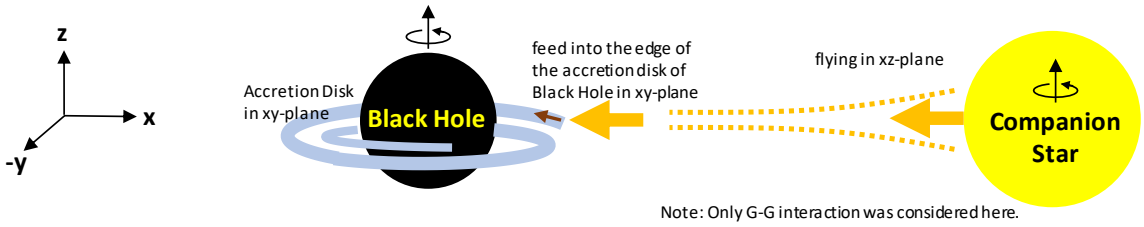

Figure 7. Illustration of the primary (or the stronger) G-G attractive (or $\overrightarrow{\mathbf{G}_r}$ to $\overrightarrow{\mathbf{G}_r}$) interaction caused matter flowing trajectory from a companion star to a black hole. The (weaker) RFg-RFg interaction (in terms of parallel spin-spin attractive interaction, or $\overrightarrow{\mathbf{G}_\varphi}$ to $\overrightarrow{\mathbf{G}_\varphi}$ interaction) was omitted here. Note: Both black hole and the companion star spin in z direction. Note: this is the same as what the artist's drawing (shown in SunQM-6s3's Fig-3a).

Example-1: That "the Moon is slowly moving away from the Earth" may be caused by the weakening the parallel spin-spin's attraction between them. Following is what I wrote in April 2022 (originally for the paper SunQM-6s2, but did not post out): "*Now I found a new explanation for why Moon is moving away from Earth, using the newly designed {N,n} QM field theory (see SunQM-6). It can be explained as that both self-spin of Earth and Moon produced RFg-forces, and these two RFg-forces attract with each other (due to the two spin have the same direction, see SunQM-6's Fig-10a, and suppose it is correct). Then the tidal force of Moon slowed down the self-spin of Earth, and the slowing self-spin of Earth produced less RFg force to attract the Moon's RFg force. Thus, the total mutual attractive force between Moon the Earth (the G-force plus the RFg-force) is decreased when the self-spin of Earth is slowed down (even the G-force is not decreasing). This caused Moon slowly moving away from Earth. If this explanation is correct, then from Earth's self-spin slow-down rate and Moon's moving away rate, we should can estimate how much RFg force is generated (or diminished) from Earth's self-spin*". Note-1: This also means, the Moon maybe have its face locked to Earth since it was born.

Example-2: As discussed in the section V, the RFg-RFg interaction in the form of the parallel spin-spin attraction between the neighboring gases/dusts/stars may have added a virtual "π-bond" to strengthen the arm's virtual chain-like structure and thus caused the abnormal fast rotation velocity of the galactical arm. If this description is correct, then, we should see that in the arm region, the majority of stars should have self-spin directions in the similar direction as that of the SMBH, and as its orbital movement direction as well as the arm's spiral-in direction. This should can be checked experimentally. Furthermore, in SunQM-3s1's section VI, during the pre-Sun ball collapsing, a pair of the (temporary) bipolar outflow is expected, and it is explained to be the nL0 effect from the Schrodinger equation's solution. According to Figure 6, those leftover fragments in the bipolar-outflow should have high percentage of opposite spin direction objects (in comparison with the spin direction of the Sun). Unfortunately it is hard to check this hypothesis in the Solar system (because its bipolar-outflow already collapsed long times ago). (Note: The nL0 effect only slow down the dynamics of the collapsing process at the two poles relative to the equator region, so that it formed a short-lived bipolar-outflow immediately after a pre-Sun ball's major collapse. After long enough time, the objects in the bipolar-outflow will be pulled back by Sun's primary G-force, and causes the bipolar-outflow to collapse). If we think the formation of the Milky Way galaxy disk is more or less the same as that of the Solar system, then we should see those old stars in the bipolar region of the galaxy may should have higher percentage of opposite spin direction (in comparison with the spin direction of the galaxy) than those in the disk plane of the galaxy. This should can be checked experimentally. Similarly, inside the Halo sphere of the Milky Way galaxy, (i.e., in the {8,1//6}o orbital shell space, see SunQM-7's Table-1), those old stars and globular clusters and even small galaxies in the bipolar region (of the Milky Way

galaxy) also should have higher percentage of opposite spin direction (in comparison with the spin direction of the Milky Way galaxy) than those in the disk plane of the Milky Way galaxy. This should also can be checked experimentally. (Note: If this is proved to be right, then it also support the hypothesis in SunQM-6s7 that Schrodinger equation/solution may already include the spin information).

Example-3: A spinning subordinate object (e.g., a companion star, or a planet) may have its matter sucked out from the two polar sites by a spinning master object (e.g., a black hole, or a star) through RFg-RFg (or the parallel spin-spin's attractive) interaction. In SunQM-6s3's Fig-3b, I used this parallel spin-spin's attraction, together with the "|nL0> elliptical/parabolic/hyperbolic orbital transition model", to explain the x-ray formation mechanism during a black hole (**BH**) pulling matter from its companion star (**CS**): "*In the {N,n} QM analysis, all matter on the surface of a star (or a planet) has the same n (and l) quantum number, although it may have different m quantum number in the |nlm> QM state description (depends on its latitude location). The self-spin QM-force of the star makes the nL0 QM state (meaning at the two pole of the star) to have the highest (orbital) energy level (relative to all other |nlm> QM states for the same n and l, see SunQM-3s1). For the (planet) Saturn, dominated by Saturn's own G/RFg-force field, this causes the (surface) mass distributed the least amount at the two pole sites (because matter wants to stay at the low orbital energy |nlm> QM state), so that it causes the significant flattening of the Saturn. However, under an outside attractive G/RFg-force filed (e.g., under the spinning BH's G/RFg-force filed), the high (orbital) energy at nL0 QM state means that the matter at the two poles of the CS is most easily given-up by the companion star's own attractive G/RFg-force. So, when a (fast spinning) BH (slowly) sucking out the mass from a (fast spinning) CS, it only sucks out the surface matter from the two poles of the star. (Note: if the BH's RFg-sucking-force is weak, then the sucked-out surface matter from CS may will form the bipolar outflow at the outside of the two poles of CS)*".

Note: A few months after I wrote down this discussion (in SunQM-6s3), I saw an online news report (https://news.creaders.net/us/2022/07/16/2505161.html) that showed the James Webb space telescope's new picture F323N (see Figure 8). See the fussy things at outside of the two poles of the Jupiter (in this picture), would it possible be the gas matter that sucked out by the Sun through Sun's and Jupiter's parallel spin-spin's attraction? (Note: Due to the Sun light/heat and the solar wind, the matter expelled from the two poles of the spinning Jupiter may will be evaporated/blown away from Jupiter and Sun. However, if there were no Sun light/heat and the solar wind, the matter expelled from the two poles of the spinning Jupiter would fly into the spinning Sun's nLL orbit, as shown in Figure 9).

According to SunQM-6s3's Fig-3a' left side and SunQM-6s3's Fig-3b' right side, I drew the Figure 9 to show (by guessing) that how a (fast spinning) black hole sucks out matter from a (fast spinning) companion start through a pure RFg-RFg interaction, or through the parallel spin-spin attraction (notice that the G-G force interaction is not included in Figure 9). Figure 9 illustrated that the companion star's fast spinning makes the nL0 mode's energy level to be high, so that it expel matter (that has opposite spin direction?) out from two poles (under the BH's strong RefSpnFrm). This matter then was driven by the primary G-force to fly to the black hole, and randomized spin direction on the way. Meanwhile, the Black hole's spin-frame makes nLL mode the lowest energy level (at the out-space of the black hole), thus forming the accretion disk (that is in nLL mode) around the black hole (at the equator of BH's RefSpnFrm). Then, when approaching to the black hole, the matter from the companion star (with the randomized spin) should be forced to go into the accretion disk (and thus in the nLL mode of BH's RefSpnFrm). Most of the matter (that sucked out from the two poles of the companion star) is feed into the accretion disk of the black hole (driven by the primary G-force, not by RFg-RFg interaction). A small part of matter (that has the opposite spin to the black hole's spin direction) in the nLL mode disk was transported to the two poles of BH's RefSpnFrm (that is in nL0 mode, or at the high energy level state) by the nL0-force and was ejected out as the bipolar outflow (but not as the astrophysical jet?).

If this explanation is correct, then the mechanism of the X-ray generation in a binary of BH-CS is still most likely to be the nL0 mode high energy expel (see SunQM-3s1's section VI, even though I was not able to mathematically prove it), not the "|nL0> Elliptical/Parabolic/Hyperbolic Orbital Transition Model". So, in my SunQM-6s3 section III's explanation-4, "*Most of the mass chunks that flying to the BH directly hit to the BH (in almost 4π solid angle directions)*" is incorrect, and the (X-ray forming) mechanism explained in SunQM-6s3's Fig-3b may have low probability to be correct (although I still like to keep it as an alternative model).

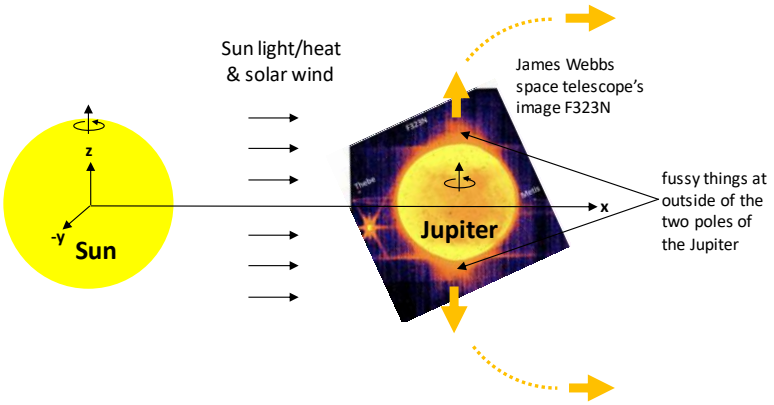

Figure 8. James Webb telescope's new picture F323N on the Jupiter, and the one possible explanation. Both self-spin directions of Sun and Jupiter are along z-axis, Jupiter's orbital plane is in xy-plane. The parallel spin-spin attraction makes spinning Sun sucking out matter from the spinning Jupiter's two polar site (in xz-plane). Picture F323N copied from: "https://www.newscientist.com/article/2328348-james-webb-space-telescope-team-quietly-releases-a-picture-of-jupiter/". Author of the picture F323N: NASA. Copyright of the picture F323N: unknown.

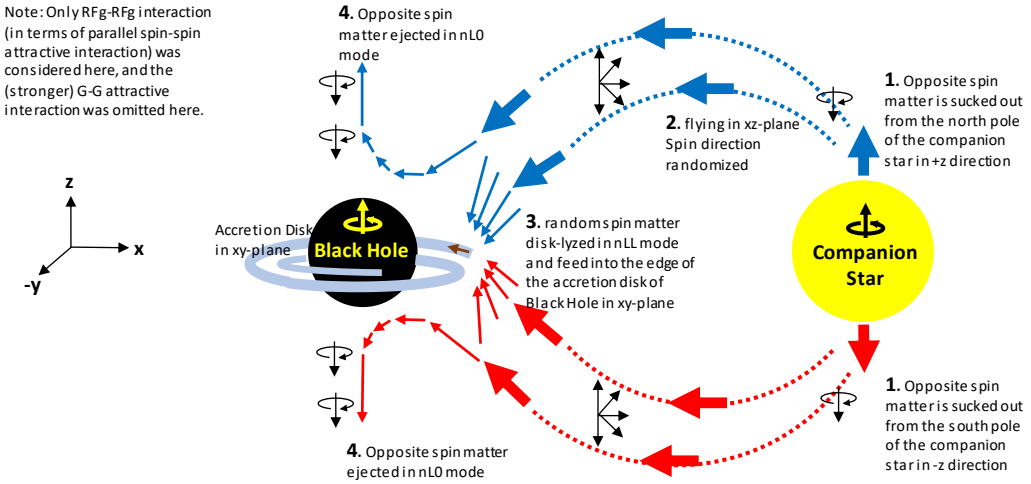

Figure 9. Illustration of the matter flow trajectory caused by a spinning black hole sucking out matter from the two poles of a spinning companion star. Only RFg-RFg interaction (in terms of parallel spin-spin attractive interaction) was emphasized here, and the (stronger) G-G attractive interaction was not emphasized here (see Figure 7 for the comparison).

V. A hypothetic mechanism on how the spiral arm of a galaxy are formed based on the "|nL0> elliptical/parabolic/hyperbolic orbital transition model"

Here is the review of the "|nL0> elliptical/parabolic/hyperbolic orbital transition model": it was originally proposed to describe the 656.1 nm photon emission process in a H-atom's electron transition from n=3 orbit to n=2 orbit (see SunQM-6s2's Fig-5b). It was explained as, when moving to the perihelion site of an n=3 elliptical orbit (in x'z'-2D plane), the n=3 orbit moving electron's (multi-shell) 3D wave packet (i.e., the "mother" particle) spins-off its outmost shell and then transit to be a n=2 orbit moving electron's (multi-shell) 3D wave packet (that moving in an n=2 elliptical orbit (also in x'z'-2D plane), i.e., the "daughter" particle). Meanwhile, the spun-off outmost shell become a (low-frequency) low-f photon (i.e., the

"newborn" particle) and emitted in the tangential direction of the elliptic orbit's perihelion site (i.e., the x' direction, because it is charge neutral and not being attracted by the proton at the center of the H-atom). The same model has also been used to describe the α-decay: inside a heavy element's nucleus there are many high energy state "virtual He-nucleus particles" (and all of them formed a single "mother" particle), then most of them (except one) de-excited to the lower QM energy state (and become a single "daughter" particle), and transfer the collective energy to the last single "virtual He-nucleus particle" and to eject it out of the heavy element's nucleus (i.e., a "newborn" particle) in (averaged) z' direction (through a parabolic orbit). Thus, the "|nL0> elliptical/parabolic/hyperbolic orbital transition model" may can be used to describe all α-, β-, γ-decays, and many other decay processes. It may even can be used to describe the gravitational wave emitted by the merging of a black hole binary (see SunQM-6s3's Fig-2, note that this gravitational wave has a spiral shape). Now I try to use the same explanation (for the two black holes merging formed (spiral) gravitational wave) to describe the formation of the two spiral arms of a galaxy.

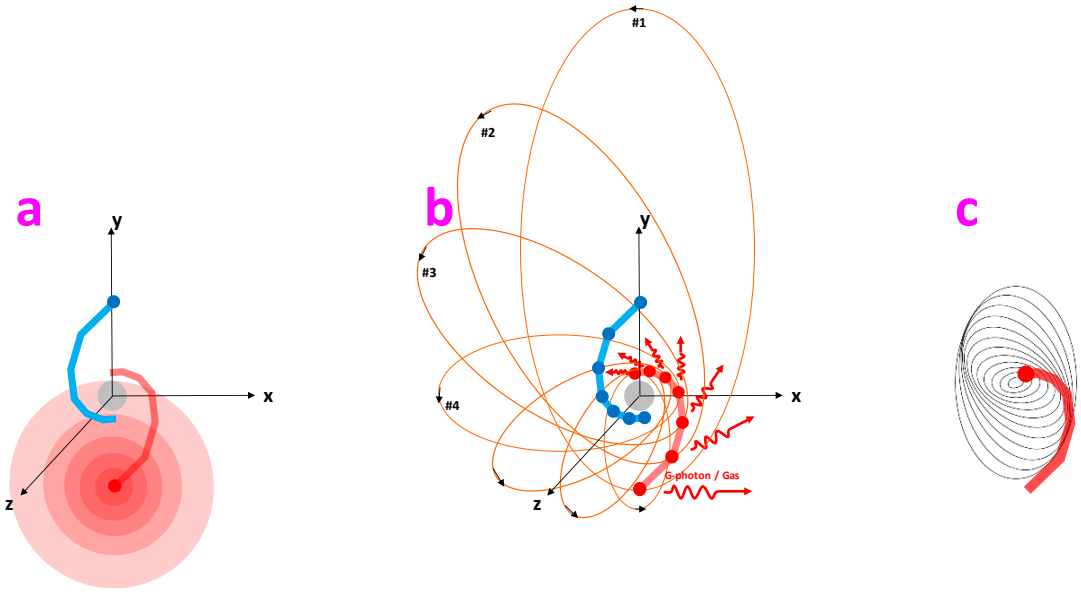

Figure 10a. A binary (the red dot and the blue dot) is doing orbital motion (in xy-plane) around the reduced mass center (at the origin) and spiraling-inward. The red dot is further depicted as a spherical 3D wave packet.
Figure 10b. The (red) spiral-in trajectory is depicted as a series of elliptical orbits that continuously decreasing the orbital quantum number n while progressing the phase in the φ-dimension (in xy-plane). The outmost shells of this spherical 3D wave packet are spun-off at the perihelion points of these elliptical orbits.
Figure 10c. Lin & Shu's model, copied from wiki "Spiral galaxy", figure "exaggerated diagram …", Author: "Mysid". Copyright: CC BY-SA 3.0.

Here is the hypothetic mechanism on how the two spiral arms of a galaxy are formed based on the "|nL0> elliptical/parabolic/hyperbolic orbital transition model". First, let's simplify the galactical formation model to be: the **supermassive center** (abbreviated as **SMC**) of the final galaxy was formed from two (equal sized) **pre-SMC** (see Figure 10, the 1st one represented by the red dot, and the 2nd one represented by the blue dot) that orbiting to each other around their reduced mass center (represented by a grey dot at the origin in Figure 10) and finally merged. The mutual orbiting and merging produced the two inward-spiral tracks, and the two pre-SMC (or their 3D wave packets) spin-off large amount of mass (the gas. dust, stars, etc., as the outmost shells of the pre-SMC 's 3D wave packets) on these two tracks, and this leftover matter formed the two spiral arms of the final new galaxy.

Following are the four similar (more detailed) explanations, using only one pre-SMC (the red dotted) as the example. Notice that the pre-SMC itself is a (spheroid, or disk) galaxy that carries large number of stars, fragments, dust and gases.

Explanation-1: As shown in Figure 10a, under the {N,n} QM description, the (red-dot) pre-SMC's core (probably also be a Supermassive Black Hole (**SMBH**) but in a smaller mass/size) become the core of one pre-SMC's 3D wave packet, the inner shells and the middle shells of the pre-SMC's 3D wave packet are composed by the large structures in the galaxy (like the arms, the stars, etc.), the outer shell and the outmost shell of the pre-SMC's 3D wave packet are composed by the minor structures in the galaxy (like the dust and gas). (Note: In the {N,n} QM mass-field theory's spherical 3D wave packet, while a large/major mass object is treated as the core of a spherical 3D wave packet, any relatively small/minor mass object (e.g., a star in a galaxy, or a Hydrogen atom in a galaxy, or the Africa continent relative to the planet Earth, etc.) that associated with this larger/major object can be treated as the outmost shell of this spherical 3D wave packet, and may can be spun-off under the "|nL0> elliptical/parabolic/hyperbolic orbital transition model"). As the (red-dot) pre-SMC doing the orbital motion around the reduced mass center, its spiral-in trajectory can be broken down into a series of elliptical orbits that continuously decreasing the orbital quantum number n while progressing the phase in the φ-dimension (in xy-plane, see #1, #2 ... elliptical tracks in Figure 10b). At the perihelion site of each elliptical orbit, the (red-dot) pre-SMC's 3D wave packet decelerated and transit to the lower n elliptical orbit, while spinning-off its outmost shell (in form of largely as the gas and dust) in the (tangential) x' direction (see Figure 10b). Subjected to the G-force attraction by the reduced mass center, these spun-off gases/dusts/stars do not follow a straight line in x' direction, but still follow the previous elliptical orbit (where the spin-off happening). (Note: that the 656.1 nm photon flies to x' direction in straight line after spin-off, because it is neutral and not subjected to the attraction of the proton in an H-atom). Thus, we have the leftover mass on a series of elliptical orbitals that have the decreasing n number and the progressing φ-phase (like Lin & Shu's model, see Figure 10c), and they formed one (red) inward-spiral arm of the galaxy (as shown in Figure 10b). (Note: In Lin & Shu's model, it may automatically produce two arms simultaneously; in my model, it only produces one arm). The second (or the blue) arm can be explained in the same way.

Explanation-2: We can also use the classical mechanics to explain the spin-off of the gases/dusts during the spiral arm formation: although all gas molecules (as a whole) are associated with the pre-SMC in motion, the gas molecules (as each individual) have its own random thermal motion on top of the pre-SMC's motion. At each time point and on each elliptical orbital's perihelion site, only small percentage (maybe less than one billionth, a purely guessed number) of the gas molecules have the exact right velocity direction and value to match to this elliptical orbit, and will be leftover to continue move on this elliptical orbit. The rest (majority) gas molecules will still associate with the pre-SMC to spiral-inward. (Note: This is exactly like that in classical mechanic explanation of the pre-Sun's quantum collapse, only a small percentage of mass that had the right moving direction at $\theta = +\pi/2$ will be leftover to be the n orbit motion mass, the majority mass (that all doing RF motion) will collapse to the lower n orbits, see SunQM-3's section I-g).

Explanation-3: Classical mechanic explanation, similar as the Explanation-2, except that, only those gas molecules that have higher than the average speed value (i.e., at the high-end of the Boltzmann distribution, also see SunQM-3's section I-g) and also have the right direction, can dissociate from pre-SMC and be leftover in the original elliptical orbit (to form the galaxy's arm).

Explanation-4: This is a {N,n} QM explanation for the Explanation-3. It is similar as that in the Explanation-1 except: at the perihelion site of each elliptical orbit, the (red-dot) pre-SMC's 3D wave packet decelerated and move to the lower n elliptical orbit (no emission of G-photon, but released the binding energy to the newborns), while the outmost shell of the pre-SMC's 3D wave packet (in the form of largely the gas and dust, etc.) collects the released binding-energy (that released by the pre-SMC and the majority of gases, see Figure 11a) and then ejects (or spins-off) in the (tangential) x' direction. Still subjected to the attraction by the reduced mass center, these spun-off gas/dust do not follow a parabolic track in the (averaged) z' direction (neither the x' direction), but still follow the previous elliptical orbit (where the ejection happening, see Figure 11b). Thus, we have the leftover mass on a series of elliptical orbitals that have the decreasing n number and the progressing φ-phase (like Lin & Shu's model, see Figure 10c), and they formed one (red) spiral-in arm of the galaxy (as shown in Figure 11c).

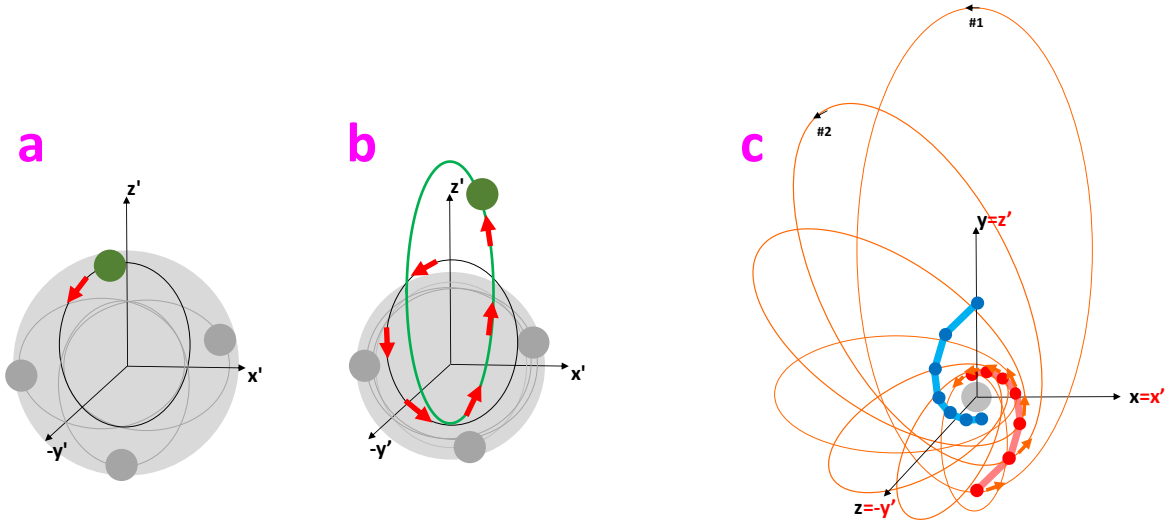

Figure 11a (and Figure 11b). Using the "|nL0> elliptical/parabolic/hyperbolic orbital model" to describe a decay process in which multiple objects (in a "mother" object) de-excited and transfer the collective energy to a single object, and then ejected this single object out of the "mother" object to become the "newborn object". Figure copied from SunQM-6s3's Fig5.
Figure 11c. Using the "|nL0> elliptical/parabolic/hyperbolic orbital model" to explain how the spiral arm of a galaxy is formed (see the Explanation-4).

All four explanations are (roughly) correct, I believed that the Explanation-4 (and the -3) is more accurate (although it is more difficult to explain and to understand). Explanation-4 (and the -3) showed the detailed mechanism on: how the transition of many objects from the high n orbit to the low n orbit, and transfer their (collective) energy to one (or a few) object and make it to the much higher n orbit (in Figure 11a and Figure 11b), or stay in the same n orbit (without further decreasing n number, see Figure 11c). Note: this is similar as the description for the α-decay, see SunQM-6s3's Fig-5).

If all gas molecules or dusts continues follow their own elliptical orbit to move, then the initial spiral arm structure produced in Figure 11c (or Figure 10c) will disappear before too long. Then, there must be an extra force that can stabilize the spiral arm structure in a galaxy. Other scientists have already put forwarded some models (the "Density wave model", the "SSPSF model", see wiki "Spiral galaxy") for the explanation.

In the chemical structure of a retinal molecule, the r-1D E-force (actually it is the residue force of the E-force) between the neighboring carbon molecules formed the "σ-bond" that provided the primary force to form the polyethylene-like (single bond) chain structure, and the π-bond provided the extra strengthen force to form the polyacetylene-like (double bond) chain structure. Based on that, Here, I am proposing a simple (conceptual) alternative hypothesis (that stabilizing the galaxy's arm structure): the r-1D G-force (actually is the residue force of the G-force) between the neighboring gas molecules/dusts/stars provided a "σ-bond" kind of primary force to stabilize the arm structure (as a chain structure), and the parallel spin-spin interaction (that belongs to the RFg-RFg interaction) between the neighboring gas molecules/dusts/stars provided a "π-bond" kind of secondary force to further stabilize the arm structure (as a chain structure). This virtual "σ-bond" and virtual "π-bond" strengthen the arm structure to be a virtual "polyacetylene-like chain". So when rotating (along the SMBH of the final galaxy), the out half of the "chain" rotates much faster than the orbital velocity produced by the pure r-1D G-force (of the final galaxy). (Note: for the RFg-RFg interaction in forms of the parallel spin-spin attraction and the virtual "π-bond" chain formation with the neighboring gas/dust/star, it may be similar as the (carbon atom's same n shell) electrons' RFe-RFe interaction in parallel spin-spin configuration when forming the sp^3 bond to the neighboring atoms (see Figure 5c), even the anti-parallel is the lower energy configuration for the non-binding carbon's same shell electrons).

This model still follows the galaxy arm's general rules like that: new stars formed in this high concentration gas region; stars that follow their own orbits can move-in or move-out of the arm, etc. Then, why we don't see the eight planets

forming arm-like structure in Solar system? That because the arm structure is stabilized by the G-force's residue force (that may show its effect at distance much larger than {5,1//6}). We can use the same model to explain the galaxy with either three, or four, or more arms, by modifying the model to be that there were three (or more) roughly equal-sized pre-SMC that orbiting with each other and then merged.

If this model is correct, then the "dark matter" is no longer "dark", it is the regular matter of cosmic gas/dust that formed a virtual chain structure, and this chain structure is formed under the residue G-force (that formed virtual "σ-bonds" among gas/dust/star) and RFg-forces (that formed virtual "π-bonds" among gas/dust/star).

Conclusion

1) For either an E/RFe-force field or a G/RFg-force field, or the spinning of a force field, we can use |n,*l*,m> QM state to describe, and then we can simplify the description by using nLL and nL0 QM modes, or even by using n=2 (with |2,1,0> and |2,1,±1>) to describe.
2) Alternatively, for a static force field (including either the G-force, or RFg-force, E-force, or RFe-force field), we can use n=1 QM state |1,0,0> to describe. When this G-force field (or RFg-force, or E-force, or RFe-force field) increase the speed of either the translational motion or the spin motion, we can use the higher n number of nLL/nL0 mode to describe.
3) The formation of the two spiral arms of a galaxy can be explained by using the "|nL0> elliptical/parabolic/hyperbolic orbital model".

Acknowledgements (of all SunQM series articles):

Many thanks to: all the (related) experimental scientists who produced the (related) experimental data, all the (related) theoretical scientists who generated all kinds of theories (that become the foundation of {N,n//q} QM theory), the (related) text book authors who wrote down all results into a systematic knowledge, the (related) popular science writers who simplified the complicated modern physics results into a easily understandable text, the (related) Wikipedia writers who presented the knowledge in a easily accessible way, the (related) online (video/animated) course writers/programmers who presented the abstract knowledge in an intuitive and visually understandable way. Also thanks to NASA and ESA for opening some basic scientific data to the public, so that citizen scientists (like me) can use it. Also thanks to the online preprinting serve vixra.org to let me to post out my original SunQM series research articles.

Special thanks to: Fudan university, theoretical physics (class of 1978, and all teachers), it had made my quantum mechanics study (at the undergraduate level) become possible. Also thanks to Tsung-Dao Lee and Chen-Ning Yang, they made me to dream to be a theoretical physicist when I was eighteen. Also thanks to Shoucheng Zhang (张首晟, Physics Prof. at Stanford Univ., my classmate at Fudan Univ. in 1978) who had helped me to introduce the {N,n} QM theory to the scientific community in 2018.

Also thanks to a group of citizen scientists for the interesting, encouraging, inspiring, and useful (online) discussions: "职老" (https://bbs.creaders.net/rainbow/bbsviewer.php?trd_id=1079728), "MingChen99" (https://bbs.creaders.net/tea/bbsviewer.php?trd_id=1384562), "zhf" (https://bbs.creaders.net/tea/bbsviewer.php?trd_id=1319754), Yingtao Yang (https://bbs.creaders.net/education/bbsviewer.php?trd_id=1135143), "tda" (https://bbs.creaders.net/education/bbsviewer.php?trd_id=1157045), etc.

Also thanks to: Takahisa Okino (Correlation between Diffusion Equation and Schrödinger Equation. Journal of Modern Physics, 2013, 4, 612-615), Phil Scherrer (Prof. in Stanford University, who explained WSO data to me (in email, see SunQM-3s9)), Jing Chen (https://www.researchgate.net/publication/332351262_A_generalization_of_quantum_theory), etc. Note: if I missed anyone in the current acknowledgements, I will try to add them in the SunQM-9s1's acknowledgements.

Reference:

[1] Yi Cao, SunQM-1: Quantum mechanics of the Solar system in a {N,n//6} QM structure. http://vixra.org/pdf/1805.0102v2.pdf （original submitted on 2018-05-03）
[2] Yi Cao, SunQM-1s1: The dynamics of the quantum collapse (and quantum expansion) of Solar QM {N,n} structure. http://vixra.org/pdf/1805.0117v1.pdf （submitted on 2018-05-04）

[3] Yi Cao, SunQM-1s2: Comparing to other star-planet systems, our Solar system has a nearly perfect {N,n//6} QM structure. http://vixra.org/pdf/1805.0118v1.pdf （submitted on 2018-05-04）
[4] Yi Cao, SunQM-1s3: Applying {N,n} QM structure analysis to planets using exterior and interior {N,n} QM. http://vixra.org/pdf/1805.0123v1.pdf （submitted on 2018-05-06）
[5] Yi Cao, SunQM-2: Expanding QM from micro-world to macro-world: general Planck constant, H-C unit, H-quasi-constant, and the meaning of QM. http://vixra.org/pdf/1805.0141v1.pdf （submitted on 2018-05-07）
[6] Yi Cao, SunQM-3: Solving Schrodinger equation for Solar quantum mechanics {N,n} structure. http://vixra.org/pdf/1805.0160v1.pdf （submitted on 2018-05-06）
[7] Yi Cao, SunQM-3s1: Using 1st order spin-perturbation to solve Schrodinger equation for nLL effect and pre-Sun ball's disk-lyzation. http://vixra.org/pdf/1805.0078v1.pdf （submitted on 2018-05-02）
[8] Yi Cao, SunQM-3s2: Using {N,n} QM model to calculate out the snapshot pictures of a gradually disk-lyzing pre-Sun ball. http://vixra.org/pdf/1804.0491v1.pdf （submitted on 2018-04-30）
[9] Yi Cao, SunQM-3s3: Using QM calculation to explain the atmosphere band pattern on Jupiter (and Earth, Saturn, Sun)'s surface. http://vixra.org/pdf/1805.0040v1.pdf （submitted on 2018-05-01）
[10] Yi Cao, SunQM-3s6: Predict mass density r-distribution for Earth and other rocky planets based on {N,n} QM probability distribution. http://vixra.org/pdf/1808.0639v1.pdf (submitted on 2018-08-29)
[11] Yi Cao, SunQM-3s7: Predict mass density r-distribution for gas/ice planets, and the superposition of {N,n//q} or |qnlm> QM states for planet/star. http://vixra.org/pdf/1812.0302v2.pdf (replaced on 2019-03-08)
[12] Yi Cao, SunQM-3s8: Using {N,n} QM to study Sun's internal structure, convective zone formation, planetary differentiation and temperature r-distribution. http://vixra.org/pdf/1808.0637v1.pdf (submitted on 2018-08-29)
[13] Yi Cao, SunQM-3s9: Using {N,n} QM to explain the sunspot drift, the continental drift, and Sun's and Earth's magnetic dynamo. http://vixra.org/pdf/1812.0318v2.pdf (replaced on 2019-01-10)
[14] Yi Cao, SunQM-3s4: Using {N,n} QM structure and multiplier n' to analyze Saturn's (and other planets') ring structure. http://vixra.org/pdf/1903.0211v1.pdf (submitted on 2019-03-11)
[15] Yi Cao, SunQM-3s10: Using {N,n} QM's Eigen n to constitute Asteroid/Kuiper belts, and Solar {N=1..4,n} region's mass density r-distribution and evolution. http://vixra.org/pdf/1909.0267v1.pdf (submitted on 2019-09-12)
[16] Yi Cao, SunQM-3s11: Using {N,n} QM's probability density 3D map to build a complete Solar system with time-dependent orbital movement. https://vixra.org/pdf/1912.0212v1.pdf (original submitted on 2019-12-11)
[17] Yi Cao, SunQM-4: Using full-QM deduction and {N,n} QM's non-Born probability density 3D map to build a complete Solar system with orbital movement. https://vixra.org/pdf/2003.0556v2.pdf (replaced on 2021-02-03)
[18] Yi Cao, SunQM-4s1: Is Born probability merely a special case of (the more generalized) non-Born probability (NBP)? https://vixra.org/pdf/2005.0093v1.pdf (submitted on 2020-05-07)
[19] Yi Cao, SunQM-4s2: Using {N,n} QM and non-Born probability to analyze Earth atmosphere's global pattern and the local weather. https://vixra.org/pdf/2007.0007v1.pdf (submitted on 2020-07-01)
[20] Yi Cao, SunQM-5: Using the Interior {N,n//6} QM to Describe an Atom's Nucleus-Electron System, and to Scan from Sub-quark to Universe (Drafted in April 2018). https://vixra.org/pdf/2107.0048v1.pdf （submitted on 2021-07-06）
[21] Yi Cao, SunQM-5s1: White Dwarf, Neutron Star, and Black Hole Explained by Using {N,n//6} QM (Drafted in Apr. 2018). https://vixra.org/pdf/2107.0084v1.pdf （submitted on 2021-07-13）
[22] Yi Cao, SunQM-5s2: Using {N,n//6} QM to Explore Elementary Particles and the Possible Sub-quark Particles. https://vixra.org/pdf/2107.0104v1.pdf (submitted on 2021-07-18)
[23] Yi Cao, SunQM-6: Magnetic force is the rotation-diffusion (RF) force of the electric force, Weak force is the RF-force of the Strong force, Dark Matter may be the RF-force of the gravity force, according to a newly designed {N,n} QM field theory. https://vixra.org/pdf/2010.0167v1.pdf (replaced on 2020-12-17, submitted on 2020-10-21)
[24] Yi Cao, SunQM-6s1: Using Bohr atom, {N,n} QM field theory, and non-Born probability to describe a photon's emission and propagation. https://vixra.org/pdf/2102.0060v1.pdf (submitted on 2021-02-11)
[25] Yi Cao, SunQM-7: Using {N,n} QM, Non-Born-Probability (NBP), and Simultaneous-Multi-Eigen-Description (SMED) to describe our universe. https://vixra.org/pdf/2111.0086v1.pdf (submitted on 2021-11-17)
[26] Yi Cao, SunQM-6s2: A Unified Description Of 1D-Wave, 1D-Wave Packet, 3D-Wave, 3D-Wave Packet, and |nlm> Elliptical Orbit For A Photon's Emission and Propagation Using {N,n} QM. https://vixra.org/pdf/2208.0039v1.pdf (submitted on 2022-08-08)
[27] Yi Cao, SunQM-6s3: Using {N,n} QM and "|nL0> Elliptical/Parabolic/Hyperbolic Orbital Transition Model" to Describe All General "Decay" Processes (Including the Emission of a Photon, a G-photon, or An Alpha-particle). (submitted on 2022-08-31, but has not been able to get posted out, I asked many times, no reply)
[28] Yi Cao, SunQM-6s4: In {N,n} QM Field Theory, A Point Charge's Electric Field Can Be Represented by Either the Schrodinger Equation/Solution, Or A 3D Spherical Wave Packet, In Form of Born Probability. https://vixra.org/pdf/2306.0136v1.pdf (submitted on 2023-06-23)
[29] Yi Cao, SunQM-6s5: Using {N,n} QM Field Theory to Describe A Propagating Photon as A 3D Spherical Wave Packet with the Oscillation Among Three QM States. https://vixra.org/pdf/2307.0098v1.pdf (submitted on 2023-07-18)
[30] Yi Cao, SunQM-6s6: Using {N,n} QM Field Theory to Study the Atomic Electron Configuration, the Pre-Sun Ball's {N,n} QM Structural Configuration, and the Nuclear Proton Configuration. https://vixra.org/pdf/2308.0118v1.pdf (submitted on 2023-08-18)
[31] Yi Cao, SunQM-6s7: The Face-to-face Tidal-locked Binary Orbital Rotation May Be the Origin of the Electron Spin and the Nucleon Spin. https://vixra.org/pdf/2310.0119v1.pdf (submitted on 2023-10-25)

[32] Douglas C. Giancoli, Physics for Scientists & Engineers with Modern Physics, 4th ed. 2009, p965, eq-36-3a.

[33] 赵凯华,陈熙谋, 电磁学（下册）, 1978, **第一版**, p311, Fig-8-17.

[34] Douglas C. Giancoli, Physics for Scientists & Engineers with Modern Physics, 4th ed. 2009, p827, eq-31-18, the "Poynting vector" $\vec{\mathbf{S}} = \frac{\mathbf{1}}{\boldsymbol{\mu_0}}\left(\vec{\mathbf{E}} \times \vec{\mathbf{B}}\right)$

[35] Douglas C. Giancoli, Physics for Scientists & Engineers with Modern Physics, 4th ed. 2009, p954.

[36] John S. Townsend, "A Modern Approach to Quantum Mechanics", 2nd ed., 2012, p498, eq-14.72.

Note: A series of SunQM papers that I am working on:
SunQM-6s9: {N,n} QM Field Theory Development On the S/RFs-force … (drafted in May. 2023).
SunQM-6s10: Schrodinger equation and {N,n} QM ... (drafted in January 2020).
SunQM-4s4: More explanations on non-Born probability (NBP)'s positive precession in {N,n}QM.
SunQM-7s1: Relativity and non-linear {N,n} QM
SunQM-9s1: Addendums, Updates and Q/A for SunQM series papers.

Note: Major QM books, data sources, software I used for SunQM series papers study:
Douglas C. Giancoli, Physics for Scientists & Engineers with Modern Physics, 4th ed. 2009.
David J. Griffiths, Introduction to Quantum Mechanics, 2nd ed., 2015.
Stephen T. Thornton & Andrew Rex, Modern Physics for Scientists and Engineers, 3rd ed. 2006.
John S. Townsend, A Modern Approach to Quantum Mechanics, 2nd ed., 2012.
Wikipedia at: https://en.wikipedia.org/wiki/
(Free) online math calculation software: WolframAlpha (https://www.wolframalpha.com/)
(Free) online spherical 3D plot software: MathStudio (http://mathstud.io/)
(Free) offline math calculation software: R
Microsoft Excel, Power Point, Word.
Public TV's space science related programs: PBS-NOVA, BBC-documentary, National Geographic-documentary, etc.
Journal: Scientific American.

Note: I am still looking for endorsers to post all my SunQM papers (including the future papers) to arXiv.org. Thank you in advance!

Note: With my 32 of SunQM papers that have been posted out so far, I believe that the framework of the {N,n} QM has been fully established. It is clear now that the {N,n} QM description is not only suitable for the mass field, but also suitable for the force field (or the energy field, etc.). Thus, my (10 years of closed-door) research phase on the {N,n} QM will end in one year (most likely in the summer of 2024). After that, I will re-write the SunQM papers (~ 35 of them) in the form of a text book. So far, my identity (for the {N,n} QM development) is: a former lecturer of Fudan University, and a current citizen scientist of California.

Appendix A. Designing experiment to detect the RFg-RFg spin-spin interaction under Earth's RefSpnFrm

Experiment-1 (a simple way): Using two exactly the same gyroscopes, (always one spins in parallel, and other spins in antiparallel to Earth's spin axis), put them on the Earth's equator and measure their weight. (Note: the spin-spin interaction between these two gyroscopes should be eliminated by separating them far enough). If the gyroscopes do not spin, then they should have the same weight; if they do spin (with the same spin speed), then they should have different weight. (Note: In SunQM-6, we expected that the parallel one is heavier than the antiparallel one). Then, we do the same measurement at every latitude and longitude and altitude (see Figure 12a), so that we can obtain the (spherical 3D map of) RFg-force on the surface (and above/near surface) of the Earth. This 3D map will help us to deduce out the analytical formula of the RFg-force field (see SunQM-6's Fig-10a).

Experiment-2 (a more complicated way): Build an oscillator with a gyroscope in it (with the spin axis of the gyroscope can be adjusted at any fixed angle to the motion of oscillation, see Figure 12b). Make two of them, the second one is always set to have the (exactly) opposite spin as that of the first one. During measurement, the motion direction of oscillation first points to the center of the Earth. By measuring the position change (and the trajectory) of the gyroscope, and the oscillation change, we may can determine the RFg-RFg spin-spin interaction force direction and strength. (Again, the spin-spin interaction between these two gyroscopes should be eliminated by separating them far enough). Notice that in this experiment, we can adjust the spin direction of the gyroscope to any direction (relative to Earth's spin direction). Plus, we

can also add a vibration to the oscillator, and adjust the speed (or even the direction) of oscillation, so that we may can measure $\vec{\mathbf{v}}$ and $\vec{\mathbf{s}}$ simultaneously.

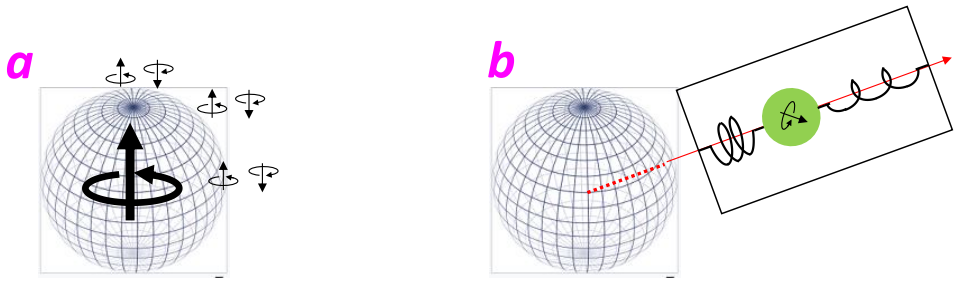

Figure 12a (left). Illustration on how to use two gyroscopes (one spins in parallel, and another spins in antiparallel, relative to Earth's spin axis) to measure the (spin value related) RFg-force on the surface (or above/near surface) of the Earth.
Figure 12b (right). Illustration on how to use an oscillator (to add $\vec{\mathbf{v}}$, with a gyroscopes in it to add $\vec{\mathbf{s}}$) to measure how the RFg-force is affected by the (relative) velocity between the two spinning objects.

Appendix B. A possible way to detect the low-f photon for an old and decaying γ ray (or x ray) photons

As mentioned in SunQM-6s2's section II-i, a 656.1 nm (f = 4.57E+14 Hz) photon's decayed low-f photon (~0.02 Hz) is undetectable (based on the current technology, because it is at sub-Hz range). However, under the Hubble constant, a gamma ray photon (e.g., 4.57E+19 Hz)'s decayed low-f photon may have the frequency in the range of ~10^3 Hz, and thus should be detectable. Thus, if we can find the 10^0 Hz ~ 10^3 Hz electromagnetic wave in a Pulsar's γ ray (or x ray) pulse signal's tail part, then we may can directly confirm the existence of the low-f photon. Furthermore, by measuring the low-f photon from different Pulsars that with different rotation speed, we may can determine the propagation speed of the low-f photon relative to the "mother" photon. (Note: We have supposed that the propagation speed of the low-f photon is a little bit slower than that of the "mother" photon).

Above is one possible way. A second possible way is that we can repeatedly calculate SunQM-6s1's Table-2 and Fig-3 for very high n, (e.g., n = 1E+3, 1E+6, 1E+9, etc.), to see whether the core and inner shells (of the spherical 3D wave packet) is moving faster than that of the out shells. This also means, to confirm whether the high frequency wave component (of a spherical 3D wave packet) is moving faster than the low frequency wave component. If is, then the same calculation will show how much faster the high frequency wave component will be than the low frequency wave component. Then, we can compare this result with the result in the Pulsar measurement.

Appendix C. In {N,n} QM, using an Oxygen atom (Z = 8) to mimic a Solar system with eight planets

In {N,n} QM, the size of the H-atom's nucleus (that equals to the size of a proton and with r_1 = 8.4E-16 meters) is at size of prot{0,1//6}, and the size of an Oxygen atom's nucleus (with r_1 = 3.15E-15 meters, see SunQM-5's Fig-2 column-8) has the size at about prot{0,2//6}, (notice that it is similar as that the Sun has the size of {0,2//6}). An atom's n=1 orbital inner size is at {-12,1//5} size, and it can fill maximum two electrons ($1s^2$) in the {-12,1//5}o orbital space. An atom's n=2 orbital inner size is at {-12,2//5} size, and it can fill maximum eight electrons ($2s^22p^6$) in the {-12,2//5}o orbital space. According to {N,n//6} QM, {-12,2//5} size equals to prot{3,2//6} size, or prot{2,12//6} size. Now suppose that we can put one electron in each following eight orbits (at the inner edge) at prot{2,18//6}, prot{2,24//6}, prot{2,30//6}, prot{2,36//6}, prot{2,72//6}, prot{2,108//6}, prot{2,144//6}, prot{2,180//6}, to mimic eight planet's orbits (i.e., Mercury {1,3//6} =

{0,18//6}, Venus {1,4//6} = {0,24//6}, Earth {1,5//6} = {0,30//6}, Mars {1,6//6} = {0,36//6}, Jupiter {2,2//6} = {0,72//6}, Saturn {2,3//6} = {0,108//6}, Uranus {2,4//6} = {0,144//6}, Neptune {2,5//6} = {0,180//6}). Then, suppose we can force all eight electrons' orbital motion in nLL mode with high n' (like that of the eight planets, see SunQM-3s11's Table-1 column-21) and in the same direction. Then this "Oxygen atom" nucleus-electron system may can mimic the Solar system in some way (even electrons are repulsive with each other).

Appendix D. A simplified "|nL0> elliptical/parabolic/hyperbolic orbital transition model"

I had proposed three kinds of "|nL0> elliptical/parabolic/hyperbolic orbital transition model": the first one is a photon emitted from H-atom in x direction (see SunQM-6s2's Fig-5b), the second one is an alpha particle emitted from an atom in the general z direction (in a parabolic/hyperbolic orbit, see SunQM-6s3's Fig-5b), and the third one is the "newborn" is emitted to stay in the original elliptical orbit while the "daughter" transits to a lower n elliptical orbit (see Figure 10b). Then, I realized that the first two models are equivalent and they are switchable (see SunQM-6s5's Fig-12 and Fig-13).

Actually these three emission model may should be merged into one: the emitted particle/object (i.e., the spin-off of the outmost shell of the 3D wave packet of the "mother particle") is always initially in x direction. For that apparently emitted in the general z direction (in either a parabolic/hyperbolic orbit, or an elliptical orbit), it is actually emitted initially in x direction, and then attracted by the center object, the direction of this newborn "low-f" particle/object is then deviated and towards to the (general) z direction. This should be able to explain SunQM-6s3's Fig-5b (alpha decay), SunQM-6s5's Fig-12 (a 0.02 Hz low-f photon is spun-off form a decaying 656.1 nm photon), SunQM-6s5's Fig-13 (an atom/molecule of H, H_2, He, H_2O, NH_3, CH_4, etc., in {1,n=1..5//6}o super shell was excited to the {2,n=1..5//6}o super shell, after the expanding of Sun's ice-evap-line), and current paper's Figure 10b.

Appendix E. A new explanation for the meaning of n in the group wave's formula $\boldsymbol{\lambda_{n,gr} = n\lambda_{1,gr}}$

Based on the knowledge of, **1)** "*the group velocity must correlate to a velocity of a group of electrons (with each electron's identity indistinguishable within the group), and the phase velocity must correlate to a velocity of each single electron (with each electron's identity is distinguishable among any of other electrons*", see SunQM-6s7's section VII-c; 2) In the phase wavelength formula of $\lambda_{n,ph} = n^2\lambda_{1,ph}$, the n^2 means that each $\lambda_{1,ph}$ represents one pair of electrons; **3)** In the standard Schrodinger equation/solution, each n shell has *l* =0..(n-1) of sub-shells (or total n number of sub-shells), and each *l* sub-shell can be treated as one sub-group, so each n shell has total n number of sub-groups; I generated a new explanation for the group wave's $\lambda_{n,gr} = n\lambda_{1,gr}$ (see SunQM-6s7's eq-6): the n in this formula means that there are n sub-groups in the n shell, and it can be presented by *l* = 0 ... (n-1) of sub-shells (or total n number of sub-shells), and each *l* sub-group (or *l* sub-shell) contains 2*l*+1 pairs of electrons (note: similar as that in SunQM-6s7's Fig-1b, but in the spherical 3D Born probability density map).

Appendix F. The "one electron in one orbit" description does not conflict with that "exploring all possible routes simultaneously"

In SunQM-6s2, instead of using the "electron cloud" description, I used the semi-classical physics' single orbital description (by using a group of elliptical orbital tracks), and narrowed the (general) QM probability description (i.e., the Copenhagen interpretation) down to the high uncertainty of the momentum vector $\Delta\vec{\boldsymbol{p}}$ at the perihelion region of the elliptical orbital track, so that an orbital motion electron can switch (within the same |n*l*m> QM state), or even transit (between

different n of |n*l*m> QM state) between the different elliptical orbital tracks at the perihelion region. This maybe appeared to un-match (or even conflict with) the principle of the quantum computing theory: the quantum computing calculates all possible ways simultaneously. After a second thought, I believed that there is no confliction: Schrodinger equation's solution is produced by interfering all possible (spherical 3D) wave modes, and then presented it as the spherical 3D wave packet (in form of BP or NBP, notice that the "wave packet" means the collection of all possible wave modes). So, in {N,n} QM description, although a single electron (in an H-atom) is moving in a single orbit at any particular time, but this single orbit (that is shown as the contour line of the density map of BP or NBP) contains all other possible wave modes' information, or, this particular orbit is the final (collective) presentation of all other possible orbits at this particular time. This description should match the principle of the quantum computing (i.e., all possible routes are explored simultaneously). Similarly, in SunQM-6s2, I explained a photon's double-slit experiment as that its out shell wave (of its spherical 3D wave packet)'s interference guided its inner core's particle motion, and this wave interference physically explored all the possible solutions simultaneously and then produced one particular solution (or route) at this particular time.

Appendix G. Why Schrodinger equation/solution can be applied to both macro-world and micro-world?

This is because the Schrodinger equation/solution only describes the point-centered (or a point-symmetric) radial radiating field (and also including the RF). So it can be used to describe any the point-centered (or a point-symmetric) radial radiating (mass, or force, or energy) field, like a Sun's point-centered mass field (or mass distribution), or a Sun's point-centered G/RFg-force field, or a Sun's point-centered gravitational potential field, or an atom's point-centered mass distribution, or an atom's point-centered E/RFe-force field, etc. However, for a chemical molecule, or a crystal structure, because their structures seriously deviated from a point-centered (or a point-symmetric) radial radiating field, they cannot be described by a simple Schrodinger equation/solution. (Also see the discussion in SunQM-1s3's section-XI).

Appendix H. We need to invent (as many as possible) very diversified QM theories for the "Feynman Pool"

The success of the {N,n} QM makes me to believe that there may should be many theories co-exist in the quantum mechanics. For example, both thermodynamics and statistic mechanics are required to describe this physical phenomena. Use only one theory would give a significant poor description than that using both theories. Furthermore, If someone could develop a pure wave based statistic mechanics (notice that the current statistic mechanics is mainly a particle-based description), then it may will give a more complete (and more understandable) describe on this physical phenomena. For a second example, both Bohr-QM and Schrodinger-QM are required to describe the {N,n} QM. Use only one theory would give a significant poor description than that using both theories. If someone could develop a pure particle based {N,n} QM, (notice that the current {N,n} QM is mostly a wave-based theory), then it may will give a more complete (and more understandable) description on the quantum mechanics. For a third example, both classical physics and {N,n} QM like to put G/RFg-force and E/RFe-force together for description (because both of G-force and E-force are proportional to 1/r^2), but QCD (Quantum Chromodynamics) likes to put S/RFs-force and E/RFe-force together for description, and from the point view of {N,n} QM, this should be no problem (because among G/RFg-force, E/RFe-force, and S/Rfs-force, you should can group any two together for description). For a forth example, to describe a human, a picture of a Santa's face may be good for the little children, a picture of a sport star may be good for the most teenaged boys, a picture of a beautiful young woman may be good for most men, a picture of a handsome and strong man may be good for most women, a human skeleton diagram may be good for medical students, etc. Only when all these pictures are presented, then we can give the best description on a human. This may also can be explained by using Richard Feynman's philosophical thought of path integral formulation: there are many possible paths from point A to point B simultaneously (and here we name it as the "**Feynman Pool**", also see SunQM-7's Appendix-G), and people always want to apply the principle of the least action on the "Feynman Pool" to get the shortest path (see the red line in Figure 13). For this purpose, first, we better to find most (if not all) paths

before we can determine which one is the shortest. Second, now I even believe that there may be no un-conditional shortest path, any shortest path is conditional, it is shortest only under this condition. The bottom-line of this discussion is, we need to find more (or as many as possible) diversified descriptions, before we can get a complete picture of the quantum mechanics. Also, because of its completeness and self-consistence, I do believe that the {N,n} QM description is qualified to be put into the "Feynman Pool" as one of the many co-existing QM theories (also see SunQM-7's Appendix-G for the discussion of the "Feynman Pool").

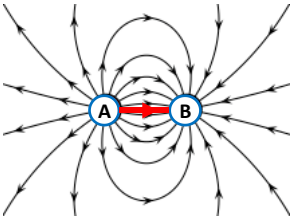

Figure 13. Illustration of many paths from point A to point B, with a shortest path in red. The collection of all the paths becomes the "Feynman Pool". Figure copied from wiki "electric field" figure "Illustration of the electric field …", and modified by me. The original Author: Geek3. Copyright: CC BY-SA 3.0.